Article

# How Can a Single Second Sphere Amino Acid Substitution Cause Reduction Midpoint Potential Changes of Hundreds of Millivolts?

Emine Yikilmaz, Jason Porta, Laurie E. Grove, Ardeschir Vahedi-Faridi, Yuriy Bronshteyn, Thomas C. Brunold, Gloria E. O. Borgstahl, and Anne-Frances Miller

*J. Am. Chem. Soc.*, **2007**, 129 (32), 9927-9940• DOI: 10.1021/ja069224t • Publication Date (Web): 12 July 2007



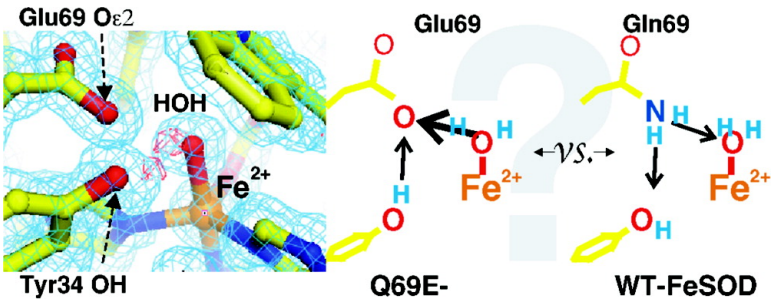


## More About This Article

Additional resources and features associated with this article are available within the HTML version:

- Supporting Information
- Links to the 7 articles that cite this article, as of the time of this article download
- Access to high resolution figures
- Links to articles and content related to this article
- Copyright permission to reproduce figures and/or text from this article

View the Full Text HTML

J|A|C|S
ARTICLES
Published on Web 07/12/2007

# How Can a Single Second Sphere Amino Acid Substitution Cause Reduction Midpoint Potential Changes of Hundreds of Millivolts?

Emine Yikilmaz,[†,‡] Jason Porta,[§] Laurie E. Grove,[||] Ardeschir Vahedi-Faridi,[§,#] Yuriy Bronshteyn,[†] Thomas C. Brunold,[||] Gloria E. O. Borgstahl,[§] and Anne-Frances Miller*[,†,‡]

*Contribution from the Department of Chemistry, University of Kentucky, Lexington, Kentucky 40506-0055, Department of Chemistry, the Johns Hopkins University, Baltimore, Maryland 21218, Eppley Institute for Research in Cancer and Allied Diseases, 987696 Nebraska Medical Center, Omaha, Nebraska 68198-7696, and Department of Chemistry, University of Wisconsin, Madison, Wisconsin 53706*

Received December 22, 2006; E-mail: afm@uky.edu

***Abstract:*** The active site metal ion of superoxide dismutase (SOD) is reduced and reoxidized as it disproportionates superoxide to dioxygen and hydrogen peroxide. Thus, the reduction midpoint potential ($E_m$) is a critical determinant of catalytic activity. In *E. coli* Fe-containing SOD (FeSOD), reduction of $Fe^{3+}$ is accompanied by protonation of a coordinated $OH^-$, to produce $Fe^{2+}$ coordinated by $H_2O$. The coordinated solvent's only contact with the protein beyond the active site is a conserved Gln residue. Mutation of this Gln to His or Glu resulted in elevation of the $E_m$ by 220 mV and more than 660 mV, respectively [Yikilmaz et al., *Biochemistry* **2006**, *45*, 1151−1161], despite the fact that overall protein structure was preserved, His is a chemically conservative replacement for Gln, and neutral Glu is isostructural and isoelectronic with Gln. Therefore, we have investigated several possible bases for the elevated $E_m$'s, including altered Fe electronic structure, altered active site electrostatics, altered H-bonding and altered redox-coupled proton transfer. Using EPR, MCD, and NMR spectroscopies, we find that the active site electronic structures of the two mutants resemble that of the WT enzyme, for both oxidation states, and Q69E-FeSOD's apparent deviation from WT-like $Fe^{3+}$ coordination in the oxidized state can be explained by increased affinity for a small anion. Spontaneous coordination of an exogenous anion can only stabilize oxidized Q69E-$Fe^{3+}$SOD and, therefore, cannot account for the *increased* $E_m$ of Q69E FeSOD. WT-like anion binding affinities and active site p*K*'s indicate that His69 of Q69H-FeSOD is neutral in both oxidation states, like Gln69 of WT-FeSOD, whereas Glu69 appears to be neutral in the oxidized state but ionized in the reduced state of Q69E-FeSOD. A 1.1 Å resolution crystal structure of Q69E-$Fe^{2+}$SOD indicates that Glu69 *accepts* a strong H-bond from coordinated solvent in the reduced state, in contrast to the case in WT-FeSOD where Gln69 *donates* an H-bond. These data and DFT calculations lead to the proposal that the elevated $E_m$ of Q69E-FeSOD can be substantially explained by (1) relief from enforced H-bond donation in the reduced state, (2) Glu69's capacity to provide a proton for proton-coupled $Fe^{3+}$ reduction, and (3) *strong* hydrogen bond acceptance in the reduced state, which stabilizes coordinated $H_2O$. Our results thus support the hypothesis that the protein matrix can apply significant redox tuning via its influence over redox-coupled proton transfer and the energy associated with it.

## Introduction

Superoxide dismutases (SODs) catalyze the disproportionation of $2\ O_2^{\bullet -} + 2\ H^+$ to $O_2 + H_2O_2$.[1−3] The FeSODs and MnSODs are highly homologous at all levels of structure[4−6] but differ from the two other families of SOD, the Cu,ZnSODs, and the NiSODs. FeSODs and MnSODs are dimers or tetramers of ∼22 kDa monomers, each with its own active site.[7] Each active site contains a single Fe or Mn ion coordinated with distorted

[†] University of Kentucky.
[‡] Johns Hopkins University.
[§] Eppley Institute for Research in Cancer and Allied Diseases.
[||] University of Wisconsin.
[#] Current address: Department of Biochemistry/Crystallography, Free University Berlin, Takustr. 6, 14195 Berlin, Germany.

(1) Lavelle, F.; McAdam, M. E.; Fielden, E. M.; Roberts, P. B.; Puget, K.; Michelson, A. M. *Biochem. J.* **1977**, *161*, 3−11.
(2) Bull, C.; Fee, J. A. *J. Am. Chem. Soc.* **1985**, *107*, 3295−3304.
(3) McCord, J. M.; Fridovich, I. *J. Biol. Chem.* **1969**, *244*, 6049−6055.
(4) Stallings, W. C.; Pattridge, K. A.; Strong, R. K.; Ludwig, M. L. *J. Biol. Chem.* **1984**, *259* (17), 10695−10699.
(5) Ringe, D.; Petsko, G. A.; Yamakura, F.; Suzuki, K.; Ohmori, D. *Proc. Natl. Acad. Sci. U.S.A.* **1983**, *80*, 3879−3883.
(6) Lah, M. S.; Dixon, M. M.; Pattridge, K. A.; Stallings, W. C.; Fee, J. A.; Ludwig, M. L. *Biochemistry* **1995**, *34*, 1646−1660.
(7) Miller, A.-F. Fe-superoxide dismutase. In *Handbook of Metalloproteins*; Wieghardt, K., Huber, R., Poulos, T. L., Messerschmidt, A., Eds.; Wiley and Sons: Chichester, 2001; Vol. 1, pp 668−682.
(8) Guex, N. *Experientia* **1996**, *52*, A26.
(9) Yikilmaz, E.; Rodgers, D. W.; Miller, A.-F. *Biochemistry* **2006**, *45*, 1151−1161.
(10) Kraulis, P. J. *J. Appl. Crystallogr.* **1991**, *24*, 946−950.

trigonal bipyramidal geometry, by two His and an $Asp^-$ in the equatorial plane, plus a third His and a coordinated solvent molecule in the axial positions (His73, His160, Asp156, and His26, Figure 1). The coordinated solvent is always present and is therefore considered part of the Fe site hereafter, while small anions that can bind in the sixth coordination site will be referred to as "exogenous" ligands.

FeSOD and MnSOD have been shown to employ a ping-pong mechanism (eq 1), which is first-order with respect to $O_2^{\bullet-}$ in both steps and in which the metal ion alternately oxidizes and reduces the substrate.[2,11,12] Therefore, the active site reduction midpoint potential ($E_m$)[97] contributes directly to the driving forces of the two half-reactions. Substrate is believed to coordinate to $Fe^{3+}$ to form a six-coordinate intermediate in reaction 1a (the 5-6-5 mechanism[13]), whereas an outer-sphere mechanism is proposed for reaction 1b.[14]

$$M^{3+}SOD(OH^-) + O_2^{\bullet-} + H^+ \rightarrow M^{2+}SOD(OH_2) + O_2 \quad (1a)$$

$$M^{2+}SOD(OH_2) + O_2^{\bullet-} + H^+ \rightarrow M^{3+}SOD(OH^-) + H_2O_2 \quad (1b)$$

where M stands for the metal ion, and the coordinated solvent molecule that normally couples proton transfer to electron transfer is in parentheses.[2,13,15]

In Fe-specific SODs from mesophiles, the coordinated solvent is engaged in hydrogen bonds (H-bonds) with the ligand $Asp^-$ and the conserved Gln69[16] (Figure 1).[6] Thus, Gln69 provides the only contact from outside the coordination sphere by which the protein can tune the p*K*'s of the coordinated solvent. Indeed, this Gln appears to be a focal point for a network of H-bonds, including the active site Tyr34, but also Trp122 in the other domain of the protein, and Asn72, all of which are highly conserved (Figure 1). Gln69 and its counterpart in MnSOD, Gln146, have been proposed to play numerous interrelated roles in support of SOD catalytic activity, including (1) relaying protons between solvent, coordinated solvent, and reactants,[17] (2) supporting ligand sphere reorganization associated with substrate binding and activation,[18,19] (3) H-bonding to bound substrate that facilitates electron transfer,[20] (4) contributing to metal ion specificity,[19,21,22] and (5) modulating the $E_m$ of the metal ion/coordinated solvent pair ($LM^{3+}(OH^-) + e^- + H^+ \Leftrightarrow LM^{2+}(OH_2)$).[23−27]

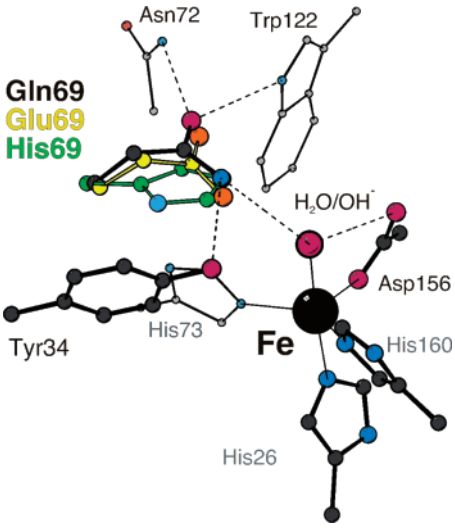


***Figure 1.*** Diagram of the active site of FeSOD showing ligands to Fe and selected second sphere residues, based on the crystallographic coordinates of WT-$Fe^{2+}$SOD (1ISA.pdb, *E. coli* numbering scheme).[6] The WT structure is depicted with gray for C, wine-red for O, and dark blue for N. In addition, the substituent His69 or Glu69 that distinguishes the mutants described in this paper is shown, as placed by overlaying each mutant active site with the WT site using swisspdbviewer,[8] based on 1ZA5.pdb and 2NYB.pdb.[9] The superpositions were calculated using the side chain atoms of residues 26, 30, 34, 73, 76 122, 156, 158, 160, and 161. Residue 69, the Fe, and the coordinated solvent were excluded. The His69 of Q69H-FeSOD is depicted with green for C and light blue for N. The Glu69 of Q69E-$Fe^{2+}$SOD is depicted with yellow for C and orange-red for O. Distant residues are depicted with lighter colors and smaller atoms. The coordinated solvent is shown twice the size of the other O atoms, near the middle of the figure, which was constructed using Molscript.[10]

Most of the active site Gln mutations described to date have been constructed in the context of MnSOD and have resulted in large decreases in catalytic activity, ranging from more than 10-fold (Q146H)[18] to more than 1000-fold (Q146E),[25] as well as shifts in metal ion specificity with respect to binding and activity[19,22,24,25] (also see Hiraoka et al.[21]). Whittaker, Edwards and co-workers have shown that mutation of Gln146 to His or Leu produces subtle changes in the absorption and magnetic circular dichroism (MCD) spectra of $Mn^{3+}$SOD, a possible coordination number change at high pH,[18] and a large decrease in affinity for $N_3^-$.[18,19] The latter is also seen for hyperthermophilic SOD employing His in place of Gln.[28] Therefore, the inactivity of Gln-to-His mutants could reflect perturbation of the electronic structure and Lewis basicity of the metal ion.

Lévêque et al. showed that the rate constants for key on-pathway steps decreased by multiple orders of magnitude upon mutation of Gln146 but concluded that proton transfer to nascent product could still occur.[25,26] However several mutants were isolated in the $Mn^{2+}$ form instead of the $Mn^{3+}$ form characteristic of WT-MnSOD, indicating an increase in the metal ion's $E_m$.[25,26] Since the $E_m$ reflects the protein's relative affinity for one oxidation state of a metal ion over another, it is interesting that mutation of Gln 69/146 has also been found to cause a

(11) Han, W. G.; Lovell, T.; Noodleman, L. *Inorg. Chem.* **2002**, *41* (2), 205−218.
(12) Fee, J. A.; McClune, G. J.; O'Neill, P.; Fielden, E. M. *Biochem. Biophys. Res. Commun.* **1981**, *100* (1), 377−384.
(13) Stallings, W. C.; Metzger, A. L.; Pattridge, K. A.; Fee, J. A.; Ludwig, M. L. *Free Radical Res. Commun.* **1991**, *12−13*, 259−268.
(14) Miller, A.-F.; Sorkin, D. L.; Padmakumar, K. *Biochemistry* **2005**, *44* (16), 5969−5981.
(15) Miller, A.-F.; Padmakumar, K.; Sorkin, D. L.; Karapetian, A.; Vance, C. K. *J. Inorg. Biochem.* **2003**, *93*, 71−83.
(16) FeSOD residues are named according to the numbering of *E. coli* FeSOD, and MnSOD residues, according to the numbering of *E. coli* MnSOD.
(17) Stoddard, B. L.; Howell, P. L.; Ringe, D.; Petsko, G. A. *Biochemistry* **1990**, *29*, 8885−8893.
(18) Edwards, R. A.; Whittaker, M. M.; Whittaker, J. W.; Baker, E. N.; Jameson, G. B. *Biochemistry* **2001**, *40* (1), 15−27.
(19) Hunter, T.; Bannister, J. V.; Hunter, G. J. *Eur. J. Biochem.* **2002**, *269*, 5137−5148.
(20) Abreu, I. A.; Rodriguez, J. A.; Cabelli, D. E. *J. Phys. Chem. B* **2005**, *109*, 24502−24509.
(21) Hiraoka, B. Y.; Yamakura, F.; Sugio, S.; Nakayama, K. *Biochem. J.* **2000**, *345*, 345−350.
(22) Bunting, K.; Cooper, J. B.; Badasso, M. O.; Tickle, I. J.; Newton, M.; Wood, S. P.; Zhang, Y.; Young, D. *Eur. J. Biochem.* **1998**, *251*, 795−803.
(23) Yikilmaz, E.; Xie, J.; Miller, A.-F.; Brunold, T. C. *J. Am. Chem. Soc.* **2002**, *124* (14), 3482−3483.
(24) Schwartz, A. L.; Yikilmaz, E.; Vance, C. K.; Vathyam, S.; Koder, R. L., Jr.; Miller, A.-F. *J. Inorg. Biochem.* **2000**, *80*, 247−256.
(25) Lévêque, V. J.-P.; Stroupe, M. E.; Lepock, J. R.; Cabelli, D. E.; Tainer, J. A.; Nick, H. S.; Silverman, D. N. *Biochemistry* **2000**, *39*, 7131−7137.
(26) Hsieh, H.; Guan, Y.; Tu, C.; Bratt, P. J.; Angerhofer, A.; Lepock, J. R.; Hickey, M. J.; Tainer, J. A.; Nick, H. S.; Silverman, D. N. *Biochemistry* **1998**, *37*, 4731−4739.
(27) Vance, C. K.; Miller, A.-F. *J. Am. Chem. Soc.* **1998**, *120* (3), 461−467.
(28) Whittaker, M. M.; Whittaker, J. W. *J. B. I. C.* **2000**, *5*, 402−408.

shift in metal-binding specificity of SOD, by Bunting et al.[22] and Hunter et al.[19]

Although the Gln mutants of MnSOD have demonstrated that Gln146 exerts an influence over the spectroscopic properties and activity of the metal ion, they have not been as informative as might have been wished, precisely because their effects are so drastic. Indeed, mutation of Gln146 to Glu results in a protein that does not bind metal ion well.[18,25] The FeSOD system, in which the active site Gln is less strongly coupled to the metal ion,[24] appears more tolerant of this mutation.[19] Thus, although the consequences of mutation may be less striking, sufficient WT-like properties are retained to permit meaningful comparison with the WT enzyme.

We have proposed that Gln146 (or Gln69) may preferentially stabilize coordinated $OH^-$ over coordinated $H_2O$ by acting as an H-bond donor to it, stabilizing the oxidized state and lowering the $E_m$.[23,24] Indeed, we found that when Gln69 in FeSOD was mutated to His, the $E_m$ rose some 220 mV. The Q69H mutant nonetheless retained 30% of WT activity on a per-Fe basis, and the tertiary structure was unchanged.[9] Mutation of Gln69 to Glu also conserved the overall structure and active site packing, based on a medium-resolution crystal structure.[9] However, this mutant displayed less than 1% of WT activity and an apparent elevation of its $E_m$ by over 660 mV, such that the protein remains fully reduced in air, in contrast to WT-FeSOD which is stable in the $Fe^{3+}$ state.[9]

In the current study we now explore the possibilities that the elevated $E_m$'s of the Q69H and Q69E mutants of FeSOD may be explained by changes in the active site H-bond network, Fe electronic structure, and/or active site charge. Electron paramagnetic resonance (EPR), nuclear magnetic resonance (NMR), and magnetic circular dichroism (MCD) spectroscopies were used to compare the active sites with respect to the coordination geometry of Fe and symmetry. Anion binding and pH titrations were performed to compare the mutants' active site charges with that of the WT enzyme. Thus, we could deduce the ionization state of residue 69. A 1.1 Å resolution crystal structure of Q69E-$Fe^{2+}$SOD was solved and provides direct evidence as to the protonation states of key active site residues and their H-bonding to each other. Taken together, these data allow us to focus on altered proton transfer and H-bonding affecting the energetics of proton transfer, rather than changes in the Fe ion's electronic structure, as primary bases for the remarkable increases in $E_m$ upon mutation of Gln69 to His or Glu. The possibility of manipulating metal ion $E_m$s over hundreds of millivolts without dramatically changing the structure has important implications for metalloenzyme design, metalloenzyme evolution, and tuning of metal ion reactivity.

## Methods

**Biochemistry.** All aspects of cloning, protein overexpression, purification, and characterization for integrity were as detailed previously (and see the Supporting Information).[9,29,30]

As described before, Q69H-FeSOD was typically isolated with only approximately 50% of the sites occupied by Fe and 30% WT specific activity on a per-Fe basis.[9] Q69E-FeSOD was much more stable and bound Fe in more than 95% of the sites, but had less than 1% of WT activity.[9,31] Q69H-FeSOD, Q69E-FeSOD, and WT-FeSOD were studied in a default buffer of 100 mM KBr, 100 mM PIPES (piperazine-*N*,*N*′-bis(2-ethanesulfonic acid)) pH 7.4, and 10% glycerol, to slow Q69H-FeSOD's loss of Fe and activity in solution and permit long spectroelectrochemical titrations. Since the high ionic strength of this buffer could attenuate anion binding and other activities of SOD, WT-FeSOD was also characterized in this buffer, to permit direct comparison between WT- and Q69H-FeSOD.

**Spectroscopy.** Optical spectra were obtained using a Hewlett-Packard 8453 UV−visible diode array spectrophotometer. SOD dimer concentrations were calculated based on the extinction coefficient at 280 nm of WT-FeSOD, $\epsilon_{280} = 10.1 \times 10^4\ M^{-1}\ cm^{-1}$,[30] and the active site Fe content was measured using the ferrozine assay[32] or by atomic absorption spectroscopy (Perkin-Elmer HP100). Specific activity was measured based on SOD's interference with reduction of cytochrome c by superoxide.[3]

EPR spectra were collected on a Bruker EMX 300 operating at X-band (9.47 GHz). The $g$ axis was calibrated at $g = 2.000$ using DPPH[33] and effective $g$ ($g_{eff}$) = 6 using myoglobin in 100 mM potassium phosphate at pH 7.8.[34] The $Fe^{3+}$ signals of the different $Fe^{3+}$-SODs were observed at a nominal power of 20 mW using 10 G modulation at 100 kHz. All samples were frozen in 4 mm tubes in the presence of 10% glycerol. The oxidized state of Q69E-FeSOD was prepared by chemical oxidation, with either $KMnO_4$ or $K_2IrCl_6$.

$^1H$ NMR spectra were collected at 400 MHz on a Varian INOVA spectrometer equipped with a 5 mm quad ($^1H$, $^{19}F$, $^{13}C$, and $^{31}P$ detection) probe at 25 °C. Non-paramagnetically relaxed resonances were substantially suppressed by saturation using the super-WEFT or the WET presequence.[29,35,36] Internal pH indicators were selectively observed in separate spin echo spectra incorporating 30 ms delays. Samples contained FeSOD at dimer concentrations of 1 to 1.4 mM.

Circular dichroism (CD) and MCD measurements at a range of temperatures were performed using a JASCO J-715 spectropolarimeter in conjunction with an Oxford Instruments SM-4000 8T magnetocryostat, and all samples contained glycerol at 55% v/v.[31,37]

**Anion Binding and pH Titrations.** Titrations of $N_3^-$ binding to 0.15 mM Q69H-$Fe^{3+}$SOD or 0.35 mM WT-$Fe^{3+}$SOD were performed at 10 °C. Apparent dissociation constants for $N_3^-$ at each pH ($K_d'$) were calculated from the dependence of the absorbance at 430 nm ($A$) on the ligand concentration [S], by fitting the data to eq 2, which describes weak binding and allows for an invariant absorbance background $B$ and additional absorbance $A_{max}$ when $Fe^{3+}$SOD is saturated with $N_3^-$:

$$A([S]) = A_{max}*[S]/(K_d' + [S]) + B \quad (2)$$

The apparent $K_d$s were corrected for the p$K$ of $HN_3 \leftrightarrow H^+ + N_3^-$ of 4.7, plotted vs pH and fit with eq 3.

$$K_d' = (1 + 10^{(pH-pK)})K_d \quad (3)$$

Equation 3 describes the case in which $N_3^-$ binds only to a protonated form of SOD, which deprotonates with a p$K$ to be determined and a dissociation constant $K_d$ or $N_3^-$ (Scheme 1).

Thus, we obtained the $K_d$ characterizing the low-pH form of SOD and the p$K$ describing the equilibrium between the two forms of SOD.

$F^-$ binding was monitored via the change in absorbance at 380 nm ($A_{380}$) at 10 °C and analyzed with eqs 2 and 3.

pH titrations of reduced Q69E- and Q69H-$Fe^{2+}$SOD were performed by NMR spectroscopic observation of an anaerobic sample adjusted

(29) Sorkin, D. L.; Miller, A.-F. *Biochemistry* **1997**, *36* (16), 4916−4924.
(30) Slykhouse, T. O.; Fee, J. A. *J. Biol. Chem.* **1976**, *251*, 5472−5477.
(31) Xie, J.; Yikilmaz, E.; Miller, A.-F.; Brunold, T. C. *J. Am. Chem. Soc.* **2002**, *124* (14), 3769−3774.
(32) Carter, P. *Anal. Biochem.* **1971**, *40*, 450−458.
(33) Wertz, J. E.; Bolton, J. R. *Electron Spin Resonance*; Chapman and Hall: New York, 1986.
(34) Gaffney, B. J.; Silverstone, H. J. *Biol. Magn. Reson.* **1993**, *13*, 1−57.
(35) Smallcombe, S. H.; Patt, S. L.; Keifer, P. A. *J. Magn. Reson. A* **1995**, *117*, 295−303.
(36) Inubishi, T.; Becker, E. T. *J. Magn. Reson.* **1983**, *51*, 128−133.
(37) Jackson, T. A.; Xie, J.; Yikilmaz, E.; Miller, A.-F.; Brunold, T. C. *J. Am. Chem. Soc.* **2002**, *124*, 10833−10845.

***Scheme 1.*** Depicting the Dissociation of $Fe^{3+}$SOD's Complex with $N_3^-$, and the Coupling of this Equilibrium to the Deprotonations of Each $HN_3$ and $Fe^{3+}$SOD (to $Fe^{3+}SOD^-$)

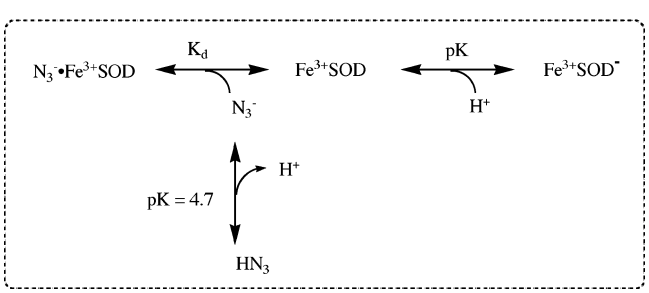


to a series of pHs with degassed 100 mM KOH and then 100 mM HCl, injected through a septum seal.[29] Proteins were first dialyzed extensively against deionized water and then transferred to an NMR tube and supplemented with $^2H_2O$ and a stock solution of NMR pH indicators, to produce a 600 $\mu$L sample. Samples contained final concentrations of ~10% $^2H_2O$ v/v, 6 mM 2,2-dimethyl-2-silapentane-5-sulfonate (DSS, the chemical shift reference), 2 mM imidazole (p$K$ = 7.10 at 25 °C), 20 mM 2,4-dimethylimidazole (p$K$ = 8.48 at 25 °C), and 1−1.5 mM SOD. Comparison of the observed chemical shifts of imidazole and dimethylimidazole with those obtained in the course of a standard pH titration, in which the pH was measured at each point using a pH electrode, enabled us to determine the internal pH of our anaerobic samples over a range of pH 5.5 to 10.[29,38] Thus, a spin echo spectrum of the pH indicators and a WEFT spectrum of the SOD active site signals were collected at each pH point in the titration. The SOD active site chemical shifts were then plotted as a function of pH and fit with eq 4, where $\delta_{AH}$ and $\delta_A$ are the chemical shifts of a resonance in the low-pH and high-pH forms, respectively.

$$\delta(\mathrm{pH}) = (\delta_{AH} + \delta_A * 10^{(\mathrm{pH}-\mathrm{p}K)})/(10^{(\mathrm{pH}-\mathrm{p}K)} + 1) \qquad (4)$$

The pH dependence of the active site $Fe^{3+}$ of Q69H-$Fe^{3+}$SOD and WT-$Fe^{3+}$SOD was monitored via EPR spectroscopy at 77 K in a cold finger. A solution of Q69H-$Fe^{3+}$SOD or WT-$Fe^{3+}$SOD in the default buffer was adjusted to successively higher pHs with 0.1 M or 0.5 M KOH and then to lower pHs with PIPES and then 1 M sodium citrate. At each point, the pH was measured using a microelectrode (Microelectrodes Inc.), and a 250 $\mu$L sample was transferred to a 4 mm EPR tube and promptly frozen in liquid $N_2$. The p$K$ characterizing the spectral changes observed was determined by plotting the derivative amplitude at $g_{eff} = 4.86$ (dA) vs pH and fitting it to a single p$K$ without cooperativity (eq 5), where $dA_{AH}$ and $dA_A$ are the fitted intensities at asymptotic low and high pH, respectively.

$$\mathrm{dA}(\mathrm{pH}) = (\mathrm{dA}_{low} + \mathrm{dA}_{high} * 10^{(\mathrm{pH}-\mathrm{p}K)})/(10^{(\mathrm{pH}-\mathrm{p}K)} + 1) \qquad (5)$$

**Calculations.** Active-site models for density functional theoretical (DFT) calculations on Q69H-FeSOD included all first-sphere ligands as well as His69 and its hydrogen bond partner Tyr34 (modeled by imidazole and 4-methyl phenol, respectively). Initial models for the oxidized and reduced states were generated using the first coordination sphere of WT-FeSOD in the appropriate oxidation state (PDB files 1ISB and 1ISA with the Asp and His ligands replaced by formate and amines, respectively) and the second sphere of Q69H-FeSOD.[9] Partial DFT energy minimizations of these models were then performed with the Amsterdam Density Functional (ADF) 2002.01 software package[39−42] using ADF basis set II, an integration constant of 3.0, and the Vosko−Wilk−Nusair[43] local density approximation along with the nonlocal gradient corrections of Becke[44] and Perdew.[45] Core orbitals were frozen through 1s (O, N, C) and 3p (Fe). For both models, the coordinates of the solvent ligand and the hydrogen atoms involved in the conserved H-bond network were DFT energy-minimized, while the coordinates of all other atoms were kept fixed. Geometries were considered converged when the maximum energy change between subsequent cycles dropped below $10^{-3}$ hartree and the maximum Cartesian gradient was less than $10^{-2}$ hartree/Å. Subsequent single-point DFT calculations were performed on these optimized active-site models using the same parameters as those employed in the geometry optimizations except that ADF basis set IV was chosen for all atoms, an integration constant of 4.0 was used, the Fe core orbitals were only frozen through 2p, and all amines were replaced by imidazoles.

***Table 1.*** Description of Data Collection[a]

| | |
|---|---|
| beamline | SSRL 11-1 |
| detector | MAR345 |
| wavelength (Å) | 0.885 57 |
| temperature (K) | 100 |
| space group | $P2_1$ |
| unit cell dimensions | $a$ = 43.51, $b$ = 107.60, $c$ = 84.12, $\beta$=94.89 |
| no. monomers in asymmetric unit | 4 |
| Matthews coefficient, $V_M$ (Å$^3$/Da) | 2.3, 47%, v/v solvent |

| X-ray data | high resolution | low resolution | combined |
|---|---|---|---|
| no. of images | 220 | 220 | |
| exposure time (s) | 60 | 6 | |
| oscillation angle, $\Delta\phi$ (deg) | 0.5 | 0.5 | |
| resolution range | na | na | 25−1.10 |
| unique reflections | na | na | 288 716 |
| completeness (%) | na | na | 87.6 (77.1) |
| mean $I/\sigma(I)$ | na | na | 28 (2.1) |
| $R_{sym}$ (%) | na | na | 2.7 (25.8) |

[a] $R_{sym} = \sum_{hkl}|<I_{hkl}> - I_{hkl}|/\sum_{hkl}I_{hkl}$. Statistics from the 1. 13 − 1.08 Å shell are in parentheses. na, not applicable (these statistics were obtained after scaling the combined data).

**Crystallography.** Crystals were grown by the hanging drop method. Rhombic crystals of Q69E-$Fe^{2+}$SOD were obtained from a 1:1 dilution of 13.7 mg/mL protein in 10 mM PIPES (pH 7.4) with a crystallization buffer of 100 mM ammonium acetate (pH 5.7), 10 mM sodium citrate, and 22.5% PEG 4000. Crystals were soaked in a cryoprotection medium made up of 80% crystallization buffer and 20% v/v ethylene glycol, mounted in a nylon loop, and then flash-cooled in liquid $N_2$.[46]

Synchrotron diffraction data were collected at the Stanford Synchrotron Radiation Laboratory (SSRL), as described in Table 1. X-ray data were processed using HKL2000.[47] The structure was solved by molecular replacement with CNS[48] using the 1.8 Å structure of *E. coli* FeSOD (1ISA)[6] as the starting model. All water molecules, dual conformers, and metal atoms were omitted from the starting model. After simulated annealing refinement the $R$ value was 32.3% ($R_{free}$ =

(38) Valcour, A. A.; Woodworth, R. C. *J. Magn. Reson.* **1986**, *66*, 536−541.
(39) Baerends, E. J.; Ellis, D. E.; Ros, P. *Chem. Phys.* **1973**, *2*, 41.
(40) Versluis, L.; Ziegler, T. J. *J. Chem. Phys.* **1988**, *88* (1), 322−328.
(41) te Velde, G.; Baerends, E. J. *J Comput. Phys.* **1992**, *99*, 84−98.
(42) Fonseca Guerra, C.; Snijders, J. G.; te Velde, G.; Baerends, E. *J. Theor. Chem. Acc.* **1998**, *99*, 391.
(43) Vosko, S. H.; Wilk, L.; Nusair, M. *Can. J. Phys.* **1980**, *58*, 1200.
(44) Becke, A. D. *J. Chem. Phys.* **1986**, *84* (8), 4524−4539.
(45) Perdew, J. P. *Phys. Rev. B* **1986**, *33* (12), 8822−8824.
(46) Rodgers, D. W. *Meth. Enzymol.* **1997**, *276*, 183−203.
(47) Otwinowski, Z.; Minor, W. DENZO and SCALEPACK. In *Crystallography of Biological Macromolecules*; Rossmann, G., Arnold, E., Eds.; Kluwer Academic Publishers: Dordrecht, The Netherlands, 2001; Vol. F, pp 226−235.
(48) Brünger, A. T.; Adams, P. D.; Clore, G. M.; DeLano, W. L.; Gros, P.; Grosse-Kunstleve, R. W.; Jiang, J. S.; Kuszewski, J.; Nilges, M.; Pannu, N. S.; Read, R. J.; Rice, L. M.; Simonson, T.; Warren, G. L. *Acta Crystallogr., Sect. D* **1998**, *54*, 905−921.

33.5%) for data between 25 and 1.5 Å resolution. Subsequent cycles of model building, isotropic *B*-value, and positional refinement to 1.1 Å resolution were performed using XtalView and Refmac5.[49,50] At this point, the $Fe^{2+}$ ions and their ligands were modeled into the active sites, and the orientations of the side chains of polar amino acids, dual conformers, and bound water molecules were modeled based on electron density $> 3\sigma$ in $F_o-F_c$ Fourier maps. Modeled water molecules that refined with *B* values above three times the average protein *B*-value were deleted. The following residues were modeled as dual conformers: (in subunit A) Ser1, Leu7, Thr22, Ile23, Glu24, Lys29, Lys43, Glu53, Glu60, Thr74, Asn83, Glu94, Ser99, Asp112, Ile115, Val136, Ser139, Asp148, Leu174, Glu175; (in subunit B) Ser1, Glu3, Lys11, Ile23, Glu24, Lys29, Lys43, Leu52, Glu53, Asn83, Glu87, Lys 91, Glu94, Ile96, Ile115, Lys 127, Ser129, Ser137, Ser139, Thr146, Asp148, Glu175, Glu184, Lys 188; (in subunit C) Ser1, Glu3, Lys11, Glu24, Lys43, Glu48, Glu53, Arg57, Ser58, Thr89, Lys91, Glu94, Lys107, Ile115, Lys132, Val136, Ser139, Glu184; and (in subunit D) Ser1, Lys11, Glu24, Lys29, Lys43, Glu53, Arg57, Glu60, Glu94, Asp112, Ser129, Glu175, Glu184, Lys188, Ala192. Occupancies of dual conformers were manually adjusted until positive and negative $F_o-F_c$ density peaks were extinguished. In the last stages of refinement, anisotropic *B* values were refined and restraints for active site bond lengths were completely relaxed. In the last cycle of refinement, Glu69 was defined as neutral (with unequal C−O bond lengths) and Glu159 was defined as anionic (with equivalent C−O bond lengths). The statistics of the resulting structure are reported in the Supporting Information, Table S1. Coordinates and structure files have been deposited and will be released upon publication of this work: PDB code 2NYB.

## Results

We have described two mutants of FeSOD in which the $E_m$ is strongly shifted from that of the WT protein: by +220 mV for Q69H-FeSOD and apparently by over + 660 mV for Q69E-FeSOD.[9] While medium-resolution crystal structures showed that active site structural changes could not be held primarily responsible, it was proposed that altered active site H-bonding might contribute to the elevated $E_m$s.[9] However the magnitudes of the redox effects were surprisingly large, calling into question whether other important mechanisms of redox tuning might not also be at work. Therefore, we now assess the possibilities that altered electronic structures, spin states, coordination numbers, and geometries for the $Fe^{2+}$ or $Fe^{3+}$ states, as well as changes in overall active site charge, might be responsible for the high $E_m$s of the mutants. As part of this effort, we also address the protonation state of residue 69 in each oxidation state and discuss the H-bonding interactions that can be invoked, along with their expected effects on the $E_m$.

**Comparison of the Reduced State $Fe^{2+}$ Electronic Structures.** NMR spectroscopy was used to compare the reduced-state active sites of the mutants and the WT enzyme, because resonances from active site hydrogens are readily identified by their fast relaxation and generally very large chemical shifts due to the nearby $Fe^{2+}$. Thus, the paramagnetic contributions to chemical shift and line width report on the covalency, active site structure, and anisotropy of unpaired electron spin density distribution (and thus the nature of the frontier orbitals).[51,52] The paramagnetically shifted resonances near 85, 42, and 36 ppm have been assigned to the $H^{N\delta1}$ hydrogens of the ligands His 26, 160, and 73, respectively.[53] Analogous resonances occur

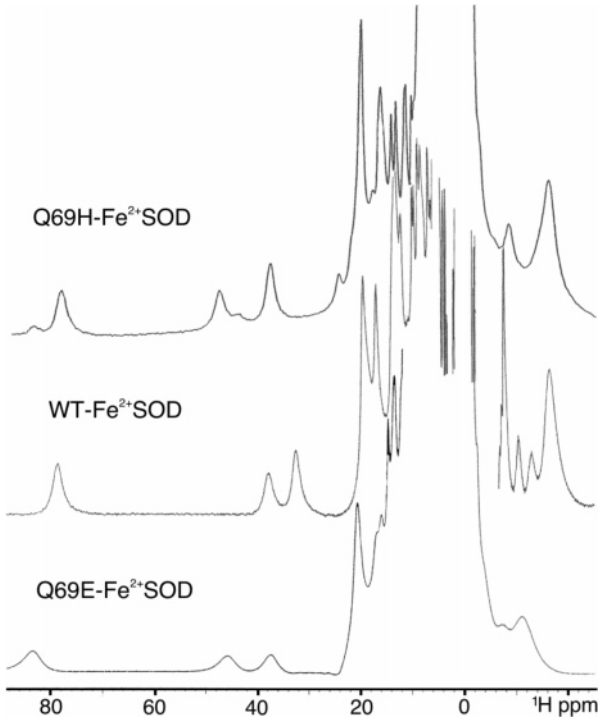


***Figure 2.*** Comparison of the NMR signals of the active sites of Q69H-, WT-, and Q69E-$Fe^{2+}$SOD. The Q69H- and WT-proteins were reduced with dithionite (see Methods section), Q69E-$Fe^{2+}$SOD was as-isolated, and all three samples were in 50 mM phosphate at pH 7.4. Data were collected at 400 MHz at 25 °C using the super-WEFT pulse sequence.[36]

at similar chemical shifts for both Q69H- and Q69E-$Fe^{2+}$SOD (Figure 2).[54,55] The recurrence of the same pattern of $H^{N\delta1}$ resonances, with similar chemical shifts in all three cases,[56] indicates that the mutations do not cause a change in the $Fe^{2+}$ spin state and suggests that they do not greatly perturb the $Fe^{2+}$ electronic structure or degree of covalency.

**Comparison of the Oxidized State $Fe^{3+}$ Electronic Structures.** The oxidized metal centers of the mutants were compared with that of the WT enzyme by EPR spectroscopy (Figure 3). EPR signals reflect the electronic configuration of $Fe^{3+}$ via the different total spins associated with different d orbital populations.[57] EPR spectra also provide information on the symmetry of the ligand field via the zero-field splitting parameters. While simulations are required to evaluate these, qualitative appraisal of the site's tendency to axial vs rhombic symmetry can be made

(49) McRee, D. E. *J. Struct. Biol.* **1999**, *125*, 156−165.
(50) Murshudov, G. N.; Vagin, A. A.; Dodson, E. J. *Acta Crystallogr., Sect. D* **1997**, *53*, 240−255.
(51) LaMar, G. N. Spin Delocalization and Electronic Structure. In *NMR of Paramagnetic Molecules*; LaMar, G. N., Horrocks, W. D., Jr., Holm, R. H., Eds.; Academic Press: New York, 1973; pp 86−127.
(52) Bertini, L.; Luchinat, C. *NMR of Paramagnetic Molecules in Biological Systems*; New York, 1986.
(53) Sorkin, D. L.; Miller, A.-F. *J. Biomol. NMR* **2000**, *17*, 311−322.
(54) Some heterogeneity was often observed in the NMR spectrum of Q69H-$Fe^{2+}$SOD as weak NMR resonances slightly offset from the main ones. These could reflect a small tendency of the His69 ring to adopt an alternate conformation in which the imidazole ring is flipped, or tautomerization.
(55) It is also evident that the Q69E-$Fe^{2+}$SOD NMR line widths are greater than those observed for the other two variants, possibly as a reflection of slower electron spin relaxation.
(56) Signals assigned to hydrogens farther from $Fe^{2+}$ have different chemical shifts in the mutants than in the WT enzyme (e.g., 20 to 12 ppm, and −6 to −15 ppm in WT-$Fe^{2+}$SOD). Resonance assignments for the mutant proteins are required before specific proposals can be made; however differences of comparable magnitude were observed upon ionization of Tyr34, indicating that they may be explained by changes in H-bonding and/or side chain packing.
(57) We can distinguish $S = {}^5/_2$ when each d orbital contains one unpaired electron and the ligand field is not strong, from $S = {}^3/_2$ or ${}^1/_2$ when there are more or stronger-field ligands.
(58) Jacobsen, C. j. H.; Pedersen, E.; Villadsen, J.; Weihe, H. *Inorg. Chem.* **1993**, *23* (7), 1216−1221.

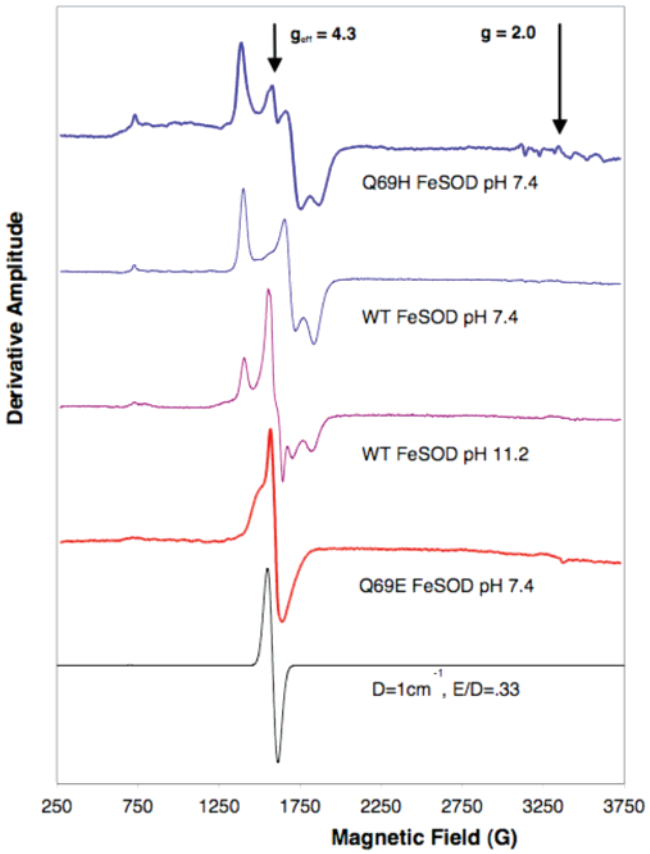


***Figure 3.*** Comparison of EPR spectra for as-isolated Q69H- and WT-$Fe^{3+}$SOD with that of chemically oxidized Q69E-$Fe^{3+}$SOD. Vertical scales were adjusted for ease of viewing. For conditions, see the Methods section. A small amount of rhombic iron at $g_{eff} = 4.3$ is released from the active site of Q69H-$Fe^{3+}$SOD, corresponding to approximately 5% of sites. The simulation of a pure rhombic site was performed using the simspc program of Weihe[58] with $g = 2.0023$, $D = 1$ cm$^{-1}$, $E/D = 0.33$, and 80 G of Gaussian line-broadening.

from the extent to which signal intensity is concentrated near an effective $g$-value of $g_{eff} = 4.31$ (rhombic limit, characteristic of an octahedral site, Figure 3, bottom) vs distributed downfield to $g_{eff} = 6$ (axial). Our data show that both mutants contain high-spin $Fe^{3+}$, like WT-$Fe^{3+}$SOD, based on the absence of signal due to $Fe^{3+}$ near $g = 2$ (characteristic of $S = {}^1/_2$). The EPR spectrum of Q69H-$Fe^{3+}$SOD is very similar to that of WT-$Fe^{3+}$SOD (Figure 3, top), indicating a pentacoordinate $Fe^{3+}$ as for WT-$Fe^{3+}$SOD, consistent with the crystal structure.[9]

The EPR signal of Q69E-$Fe^{3+}$SOD suggests a six-coordinate $Fe^{3+}$, based on the signal's relatively small deviation from rhombicity (Figure 3, compare with the simulated perfectly rhombic signal). This significant departure from neutral-pH WT-$Fe^{3+}$SOD suggests either a change in coordination mode of the $Asp^-$ ligand to bidentate,[59] or coordination of an exogenous anion in the sixth coordination site.[60] Since all crystal structures of $Fe^{3+}$SOD to date have determined that the $Asp^-$ ligand is coordinated via only one O, a change to bidentate $Asp^-$ coordination seems less likely than acquisition of an exogenous ligand. In Q69E-$Fe^{2+}$SOD, the $Fe^{2+}$ remains five-coordinate (above); thus, binding of the proposed exogenous ligand is specific to the $Fe^{3+}$ state.

MCD spectra of Q69E-$Fe^{3+}$SOD collected at several pH values revealed an increasing population of a five-coordinate species at low pH, supporting exogenous $OH^-$ as a sixth ligand at neutral pH. Importantly, the five-coordinate species that was more prominent at lower pH exhibited similar MCD features to WT-$Fe^{3+}$SOD at neutral pH, and the neutral-pH species of Q69E-$Fe^{3+}$SOD displayed similar MCD features to high-pH WT-$Fe^{3+}$SOD (not shown).[23,37] Indeed, the neutral pH EPR spectrum of Q69E-$Fe^{3+}$SOD is more similar to the rhombic signal that becomes prominent in the spectrum of WT-$Fe^{3+}$-SOD at high pH (Figure 3, middle). Finally, $N_3^-$ binding to Q69E-$Fe^{3+}$SOD produced a very similar EPR spectrum to that shown in Figure 3, and the $N_3^-$ complex has been shown to be six-coordinate based on MCD spectroscopy.[6,31,61] Together, these findings indicate that Q69E-$Fe^{3+}$SOD has an exogenous anion bound, which is likely $OH^-$, and that the coordination number, geometry, and electronic structure of Q69E-$Fe^{3+}$SOD at neutral pH are similar to those of WT-$Fe^{3+}$SOD at high pH, while Q69E-$Fe^{3+}$SOD at very low pH resembles WT-$Fe^{3+}$SOD at neutral pH.

**Insight into Active Site Charge.** WT-FeSOD's tight coupling between proton uptake and metal ion reduction results in no net change in charge upon metal ion reduction,[2] which argues that there should not be a large Coulombic contribution to redox tuning even if residue 69 were charged. However, the different oxidation states of Fe are expected to be associated with different charge *distributions*: $Fe^{3+}$-$OH^-$ vs $Fe^{2+}$-$OH_2$. Due to the close proximity of residue 69, coordinated $OH^-$ would be stabilized by the imidazolium form of histidine but destabilized by glutamate at this position (Figure 1). Therefore, it is important to assess whether residue 69 might be ionized.

The proximity of His69 or Glu69 to Fe makes it difficult to determine their protonation states via NMR methods, due to paramagnetic effects. However, we can assess the ionization state of residue 69 indirectly, because ionization would cause the active site to have a different net charge than that of the WT enzyme, in which Gln69 is always neutral. Thus, if His69 were ionized in the oxidized state, its positive charge should enhance the active site's affinity for anions including $OH^-$ (lowering the oxidized active site p*K*), and if it were ionized in the reduced state it should stabilize the tyrosinate form of Tyr34, thus lowering the reduced state active site p*K*.[62] Conversely, if Glu69 were ionized in the oxidized state it should disfavor anion binding and raise the p*K* associated with binding of $OH^-$, and if it were ionized in the reduced state it would suppress formation of tyrosinate 34 and raise the associated p*K*. Therefore, we have assessed the mutant active sites' propensities to bind anions and undergo deprotonation.

*Anion binding affinities of Q69H-$Fe^{3+}$SOD:* Treatment of Q69H-$Fe^{3+}$SOD with $F^-$, $N_3^-$, or $OH^-$ resulted in EPR and optical spectra that resemble those observed for WT-$Fe^{3+}$SOD, suggesting formation of inner-sphere complexes analogous to those of the WT enzyme. Titrations of $N_3^-$ binding to Q69H-$Fe^{3+}$SOD were performed over a range of pH values, by monitoring absorbance at 430 nm, which is characteristic of the $N_3^-$ complex of Q69H- or WT-$Fe^{3+}$SOD (Figure 4A). $N_3^-$ was found to bind more weakly to Q69H-$Fe^{3+}$SOD at high pH, as

(59) Lee, D.; Lippard, S. J. *Inorg. Chem.* **2002**, *41* (10), 2704−2719.
(60) Coordination of Glu69 as a sixth ligand is excluded by our crystal structures. Yikilmaz, et al. *Biochemistry* **2006**, *45*, 1151−1161.
(61) Tierney, D. L.; Fee, J. A.; Ludwig, M. L.; Penner-Hahn, J. E. *Biochemistry* **1995**, *34*, 1661−1668.
(62) Sorkin, D. L.; Duong, D. K.; Miller, A.-F. *Biochemistry* **1997**, *36*, 8202−8208.

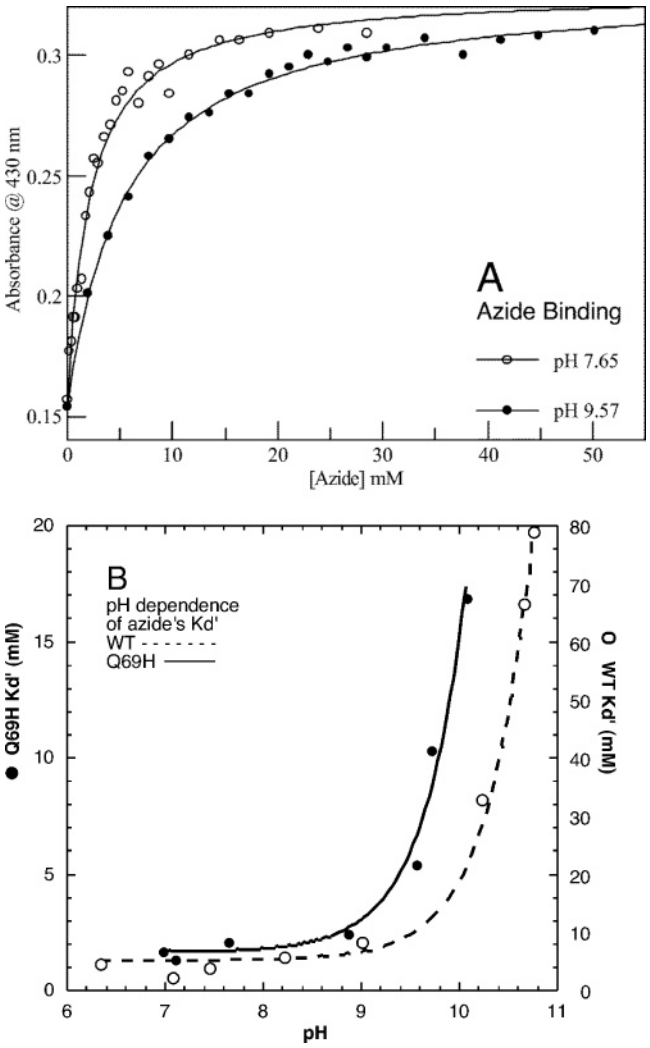


***Figure 4.*** (A) Optical titrations of $N_3^-$ binding to Q69H-$Fe^{3+}$SOD and (B) pH dependence of the obtained apparent $K_d$'s after correction for the p*K* of $N_3^-$, compared to that of WT-$Fe^{3+}$SOD. Data in panel A are accompanied by plots of eq 2 incorporating the best-fit values for $K_d'$ of 2.3 and 5.5 mM obtained at pH 7.65 and 9.57, respectively. Data in panel B are accompanied by plots of eq 3 incorporating best-fit values of $K_d$ ($K_{d,Q69H}$ = 1.7 mM and $K_{d,WT}$ = 5.5 mM for Q69H- and WT-$Fe^{3+}$SOD, respectively) and p*K* (9.1 and 9.6 for Q69H- and WT-$Fe^{3+}$SOD, respectively). Please note different vertical scales for WT- and Q69H-$Fe^{3+}$SOD data, in panel B.

observed previously for the WT enzyme.[2] For each pH, the apparent dissociation constant ($K_d'$) for $N_3^-$ was corrected as needed for protonation of $N_3^-$, using $HN_3$'s p*K* of 4.7. The corrected $K_d$'s were then plotted as a function of pH and fit with eq 3 for anion binding to the low-pH form present in a pH equilibrium (Figure 4B, and see the Methods section). The excellent agreement with the model indicates either competition with $OH^-$ binding or a requirement for proton uptake upon anion binding.[63] The resulting $K_d$ for $N_3^-$ of 1.7 mM (at low pH) and p*K* of 9.1 characterizing inhibition of $N_3^-$ binding, are comparable to the WT-FeSOD $K_d$ for $N_3^-$ of 5.5 mM and p*K* of 9.6, respectively (Table 2).

We also characterized the pH dependence of Q69H-$Fe^{3+}$-SOD's optical and EPR spectral signatures. As observed for WT enzyme, some loss of active site $Fe^{3+}$ was evident at high

(63) Whittaker, M. M.; Whittaker, J. W. *Biochemistry* **1997**, *36*, 8923−8931.
(64) Fee, J. A.; McClune, G. J.; Lees, A. C.; Zidovetzki, R.; Pecht, I. *Isr. J. Chem.* **1981**, *21*, 54−58.

***Table 2.*** Comparison of Anion Binding and p*K*'s of Q69H-FeSOD and WT-FeSOD[a]

| property/SOD type | WT-$Fe^{3+}$SOD | Q69H-$Fe^{3+}$SOD |
|---|---|---|
| p*K* of oxidized active site | 10.5 ± 0.4[b] | 9.3 ± 0.1 |
| apparent p*K* affecting activity | 8.8[c] | 8.8 ± 0.4 |
| $K_d$ for $N_3^-$ at low pH | 5.5 ± 1.2 mM[b] | 1.7 ± 0.5 mM |
| p*K* affecting $N_3^-$ binding | 9.6 ± 0.11[b] | 9.1 ± 0.15 |
| $K_d$ for $F^-$ (low pH) | 6.9 mM[d] | 3.0 ± 0.3 mM |
| p*K* of the reduced active site | 8.5 ± 0.1[e] | 9.1 ± 0.1 |

[a] Samples were suspended in the default buffer augmented by $N_3^-$ or $F^-$, or adjusted to higher pH as required. [b] These values for WT-$Fe^{3+}$SOD were obtained in the default buffer of 100 mM KBr, 100 mM PIPES, and 10% glycerol, for consistency with the p*K* listed in the same line for Q69H-$Fe^{3+}$SOD. In low ionic strength phosphate buffer, we measured a WT-$Fe^{3+}$SOD p*K* of 9.1, in excellent agreement with literature values ranging from 8.6 to 9.[2,12,64] [c] Taken from Fee et al.[12] [d] Taken from Bull and Fee.[2] [e] Taken from Sorkin et al.[29]

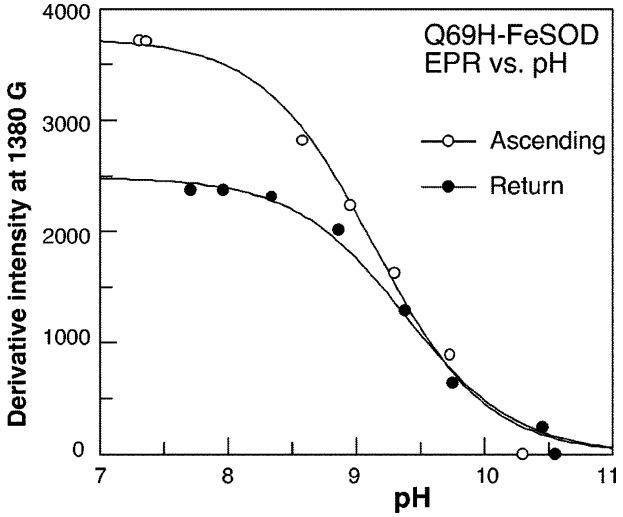


***Figure 5.*** pH titration of Q69H-$Fe^{3+}$SOD monitored by EPR spectroscopy. The EPR derivative intensity of the feature at $g_{eff}$ = 4.8 (1380 G) as a function of pH in the ascending titration (○) and in the reverse titration back to neutral pH (●).

pH, and the signal of the released $Fe^{3+}$ was similar to that of the high-pH state. Therefore, we monitored the amplitude of the EPR signal of the neutral-pH state at 1380 G, which yields substantially reversible titrations (Figure 5). The p*K* associated with the equilibrium between the two EPR species was 9.3 for Q69H-$Fe^{3+}$SOD, vs a p*K* of 10.5 for WT-$Fe^{3+}$SOD in the same buffer. The close agreement between the p*K*s associated with the EPR signals and inhibition of $N_3^-$ binding suggests that the same event is responsible for both in Q69H-$Fe^{3+}$SOD, as was also seen for in WT-$Fe^{3+}$SOD (Table 2).[2,12,30]

The fact that Q69H-$Fe^{3+}$SOD's p*K* for $OH^-$ binding and its $K_d$s for $F^-$ and $N_3^-$ binding are similar to those of WT-$Fe^{3+}$-SOD (Table 2) suggests similar $Fe^{3+}$ Lewis acidity and similar electrostatic environments in the two active sites. Therefore, we conclude that His69 in Q69H-$Fe^{3+}$SOD is neutral like Gln69 in the WT protein.

**Ionization State of His69 in Reduced Q69H-$Fe^{2+}$SOD.** NMR-detected pH titrations of Q69H-$Fe^{2+}$SOD revealed an active site p*K* of 9.1 ± 0.1, associated with changes in the ligand His $H^{\delta 1}$ NMR resonance positions that are similar to those observed in WT-$Fe^{2+}$SOD upon ionization of Tyr34 (Figure 6).[29] Therefore, by analogy to WT-$Fe^{2+}$SOD,[15,62] the active site p*K* of Q69H-$Fe^{2+}$SOD is likely also due to ionization of Tyr34. The fact that the p*K* value is not changed much, from 8.5 in

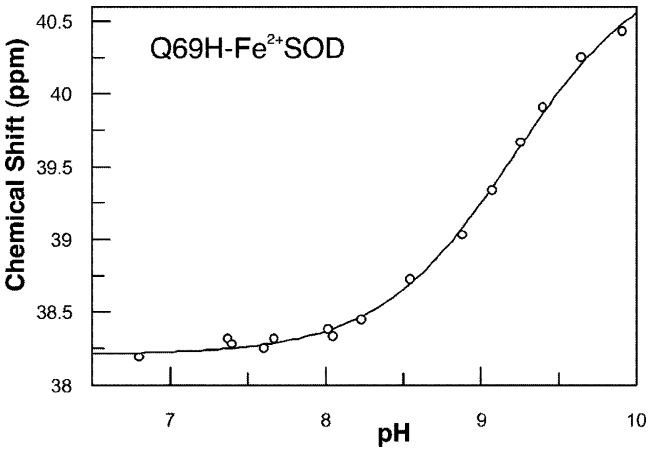


***Figure 6.*** Example of the pH dependence of a Q69H-$Fe^{2+}$SOD active site resonance ($H^{\delta 1}$ of His73). The titration was performed anaerobically as described in the Methods section. The data are accompanied by the best fit of eq 4, with p$K$ = 9.2.

WT-$Fe^{2+}$SOD to 9.1 in Q69H-$Fe^{2+}$SOD, argues that in the reduced state, too, His69 is neutral like the Gln it replaces.

**Support from DFT Calculations.** DFT computations based on crystallographic coordinates[9] agree with the above experiments in concluding that His69 is neutral, not positively charged. For neutral His69, protonation at $N^{\epsilon 2}$ (facing coordinated solvent) is calculated to be only slightly favored over protonation at $N^{\delta 1}$ in the oxidized state (by 10 kJ/mol). Thus, either polarity of His69 would appear energetically reasonable, and His69 could act as either an H-bond acceptor or donor to coordinated $OH^-$. This constitutes a shift from the case of Gln69, which is exclusively a hydrogen bond donor to coordinated solvent, as its H-bond from Trp122 engages the $C^{\delta}{=}O^{\epsilon 1}$ and constrains the $N^{\epsilon 2}H_2$ group to face coordinated solvent (Figure 1). Analogous H-bonds to Trp122 and Asn72 are absent for the Q69H-FeSOD mutant.[9]

In the reduced state, the experiments indicate neutral His69 and calculations indicate protonation exclusively at the $N^{\delta 1}$ position, which we calculate to be 45 kJ/mol more favorable than protonation at $N^{\epsilon}$ that faces coordinated solvent. His69's p$K$ for protonation of the second N must be depressed below 6, since our NMR-detected pH titrations did not reveal any spectral changes at low pH other than those accounted for by deprotonation of Tyr34. Neutral His69 could be stabilized by H-bond donation from coordinated $H_2O$ and the nearby charge of the $Fe^{2+}$ site.

**Ionization State of Glu69 in Q69E-FeSOD.** As noted above, Q69E-$Fe^{3+}$SOD's and $N_3^-$·Q69E-$Fe^{3+}$SOD's EPR signals are indicative of exogenous anion binding to $Fe^{3+}$.[65] However, Q69E-$Fe^{3+}$SOD's affinity for $N_3^-$ could not be measured because it was not experimentally possible to produce a stable five-coordinate state, as a starting point for titrations. This impediment is nonetheless informative, as it shows that a pentacoordinate WT-like Q69E-$Fe^{3+}$SOD state is quite unfavorable and that the oxidized state of the mutant is significantly *stabilized* by spontaneous coordination of some anion. This finding also argues against Glu69 being negatively charged in oxidized Q69E-$Fe^{3+}$SOD.

In reduced Q69E-$Fe^{2+}$SOD, NMR experiments indicate that Glu69 is anionic. Paramagnetically shifted $^1$H NMR resonances did not display any dependence on pH between pH 6.8 and 9.8, in contrast with Q69H- and WT-$Fe^{2+}$SOD (supplemental Figure S1).[66] Thus, either Tyr34's p$K$ is lower than 5.8 or it is greater than 10.8. Our high-resolution crystal structure indicates that Tyr34 is fully protonated at pH 5.7 (see below), so Tyr34's p$K$ is >10.8, as opposed to 8.5 in WT-$Fe^{2+}$SOD. This increase suggests that Glu69 is ionized, as the extra negative charge this would place next to Tyr34 would disfavor Tyr34 ionization, consistent with our data.

The high-pH paramagnetically shifted NMR spectra of Q69E-$Fe^{2+}$SOD also differed from those of WT-$Fe^{2+}$SOD in that the $H^{\delta 1}$ of His160[53] exchanged rapidly with solvent in WT-$Fe^{2+}$-SOD[29] but not in Q69E-$Fe^{2+}$SOD. In WT-$Fe^{2+}$SOD, the His160 $H^{\delta 1}$ ultimately becomes resistant to solvent exchange at very high pH upon ionization of Tyr34, and this was interpreted to reflect repulsion of the exchange catalyst $OH^-$ by anionic tyrosinate 34.[34,62] Thus, suppression of exchange in the Q69E-$Fe^{2+}$SOD active site supports the presence of anionic Glu69. The reduced-state Q69E-$Fe^{2+}$SOD active site charge therefore appears to be significantly different from that of the WT enzyme, and we propose that Glu69 is anionic in this case.

**Protonation States in Reduced Q69E-$Fe^{2+}$SOD: New Insights from a 1.1 Å Resolution Crystal Structure.** The protonation state of Glu69 in the reduced state was also assessed by analysis of a high-resolution crystal structure of Q69E-$Fe^{2+}$-SOD. This structure was refined to $R$ = 15.9% (17.4% $R_{free}$) and a 1.1 Å resolution with an estimated overall coordinate error of 0.020−0.033 Å (ESU based on maximum entropy and free $R$, supplemental Table S1, Table 1). The quality of the data distinguished two conformations for several residues, but the new structure's general features and active site structure are entirely consistent with previous results[9] (supplemental Figures S2 and S3).[67] Thus we observe the signature pentacoordinate Fe bound by three His and one $Asp^-$ in addition to the coordinated solvent discussed above. Bond distances are listed in Table 3 and compare well with those published based on an intermediate-resolution structure of Q69E-$Fe^{2+}$SOD; however, the standard deviations between distances measured in the four different active sites per unit cell are much smaller in the 1.1 Å structure (Table 3 and supplemental Figure S3). This improvement is particularly important for discriminating between possible protonation states.[68]

The $Fe{-}O_{CoordSolv}$ distance supports $Fe^{2+}$ coordinated by $H_2O$, as opposed to $Fe^{3+}$ coordinated by $OH^-$. Specifically, our average $Fe{-}O_{CoordSolv}$ distance based on the four active sites per unit cell is 2.16 (2) Å,[69] close to the average $Fe{-}O_{CoordSolv}$ distance of 2.11 (5) Å obtained for 87 $Fe^{2+}{-}OH_2$ compounds in the Cambridge Structural Database (CSD), and much farther from the average value of 2.03 (9) Å obtained for 94 $Fe^{3+}{-}OH^-$ compounds. The CSD contained so few $Fe^{2+}{-}OH^-$ compounds analogous to the FeSOD active site that we could not assess this possibility with confidence.[70] However, the fact that some 95% of the $Fe^{2+}$compounds with coordinated water were reported with the latter as $H_2O$ instead of $OH^-$ indicates

(65) Detailed MCD, EPR, and computational analyses of these mutants' Fe sites will be published separately.

(66) Based on our experience with other mutants, it seems less likely that deprotonation of Tyr34 is occurring but not affecting any of the paramagnetically dispersed resonances.

(67) The rmsd between backbone heavy atoms of the 1.6 Å structure and the 1.1 Å structure is 0.4 Å.

(68) Although we were not able to resolve discrete density for labile protons in the active site, aliphatic (nonexchangable) H atoms were visible on side chains in numerous areas of the structure.

(69) Averaged over four sites per crystallographic unit cell.

(70) 4 structures were identified of which 2 were suspect.

***Table 3.*** Active Site Bond Lengths and Hydrogen Bond Distances of Q69E-$Fe^{2+}$SOD

| | Q69E-$Fe^{2+}$SOD at 1.1 Å; in Å (2NYB.pdb)[a] | Q69E-$Fe^{2+}$SOD at 1.6 Å; in Å (2BKB.pdb)[a,b 9] | wild-type $Fe^{2+}$SOD at 1.8 Å; in Å (1ISA.pdb)[c] |
|---|---|---|---|
| | A. Covalent Bonds (Å) | | |
| $Fe-N^{\epsilon 2}{}_{His26}$ | 2.204 (0.011) | 2.235 (0.051) | 2.185 (0.007) |
| $Fe-N^{\epsilon 2}{}_{His73}$ | 2.111 (0.018) | 2.155 (0.059) | 2.045 (0.025) |
| $Fe-O^{\delta 2}{}_{Asp156}$ | 1.942 (0.009) | 1.955 (0.013) | 1.937 (0.022) |
| $Fe-N^{\epsilon 2}{}_{His160}$ | 2.126 (0.011) | 2.138 (0.056) | 2.121 (0.011) |
| $Fe-O_{CoordSolv}$[d] | 2.164 (0.022) | 2.138 (0.046) | 2.044 (0.023) |
| | B. Hydrogen Bonds (Å) | | |
| $O_{CoordSolv} \cdots O^{\delta 1}{}_{Asp156}$ | 3.19 (0.019) | 3.33 (0.036) | 2.88 (0.12) |
| $O^{\epsilon 2}{}_{Glu69} \cdots O_{CoordSolv}$ | 2.784 (0.009) | 2.81 (0.073)) | 3.42 (0.00)) |
| $O^{\epsilon 2}{}_{Glu69} \cdots O^{\zeta}{}_{Tyr34}$ | 2.782 (0.044) | 2.73 (0.074) | 3.11 (0.00) |
| $O^{\epsilon 1}{}_{Glu69} \cdots N^{\delta 2}{}_{Asn72}$ | 3.157 (0.058) | 3.21 (0.060) | 3.31 (0.05) |
| $O^{\epsilon 1}{}_{Glu69} \cdots N^{\epsilon 1}{}_{Trp122}$ | 2.852 (0.025) | 2.90 (0.073) | 3.08 (0.04) |

[a] For Q69E-$Fe^{2+}$SOD, average values were calculated over the four monomers in the asymmetric unit; standard deviations are enclosed by parentheses. [b] Although the 1ISA coordinates represent the highest resolution WT structure currently available in the PDB,[6] the resolution is significantly lower than that of our current Q69E-$Fe^{2+}$SOD structure. Therefore, data from another Q69E-$Fe^{2+}$SOD structure[9] of resolution comparable to that of the WT are also provided. [c] For WT-$Fe^{2+}$SOD, values are the averages of the distances found for the two monomers in the asymmetric unit. Also, residue 69 is a Gln, rather than a Glu, but the analogous distances are presented. [d] Coordinated solvent was modeled using atomic scattering factors for O. The methods used to refine the structure did not include any use of charge for this group.

that $H_2O$ is the more chemically reasonable assignment. Notably, the published WT-$Fe^{2+}$SOD structure reports an $Fe^{2+}-O_{CoordSolv}$ distance of 2.04 (2) Å (Table 3). This raises the possibility that the Fe centers in that WT-$Fe^{2+}$SOD structure (1ISA) were not fully reduced by the dithionite treatment applied to the crystals.[6] Q69E-$Fe^{2+}$SOD is reduced as-isolated, so its crystals were grown from material that was already fully in the $Fe^{2+}$ state.

The distance between the O of coordinated solvent and the nearby $O^{\epsilon 2}$ of Glu69 is considerably shorter than the analogous $N^{\epsilon}-O_{CoordSolv}$ distance in WT-$Fe^{2+}$SOD (2.8 Å vs 3.4 Å, respectively, Table 3B). Glu69's distances to Tyr34 and Trp122 are also significantly shorter than the analogous distances in WT-$Fe^{2+}$SOD, indicating a general tightening of the H-bonding network involving residue 69, as observed previously in the 1.6 Å resolution crystal structure.[9] Not all H-bond distances are shorter, though; the distance between coordinated solvent and the noncoordinated $O^{\delta 1}$ of Asp156 is significantly longer than that in WT-$Fe^{2+}$SOD, indicating that Glu69 draws coordinated solvent to itself (whereas Gln69 may even repel it[23] but see Rulisek and Ryde[71]). A similar shift in the placement of coordinated solvent between Asp156 and the active site Gln or its mutational replacements has been observed in MnSOD by Edwards et al.[18]

The protonation states of Tyr34 and Glu69 could be determined from the C—O distances of their side chains. Tyr34 appears to be neutral based on the C—O distance of 1.38 Å, which would be shorter than 1.30 Å for tyrosinate. Similarly, C—O distances distinguish carboxylate from neutral carboxylic acid. For carboxylates, equal C—O distances of 1.25 (1) Å are expected, whereas for carboxylic acid C—OH and C═O distances of 1.31 (2) Å and 1.22 (2) Å are expected, respectively, based on a survey of 176 compounds in the CSD.[72]

(71) Rulisek, L.; Ryde, U. *J. Phys. Chem. B* **2006**, *110*, 11511−11518.

***Table 4.*** C−O Bond Lengths Obtained from Refinement of the Q69E-$Fe^{2+}$SOD Structure Assuming Either Anionic or Neutral Glu69 (Distances in Å)[a]

| assumption → residue ↓ | anionic glutamate ∼$COO^-$ | neutral glutamic acid ∼COOH | interpretation |
|---|---|---|---|
| $Glu69C^{\delta}-O^{\epsilon 1}$ | 1.248 (0.003) | 1.237 (0.019) | intermediate, C═O |
| $Glu69C^{\delta}-O^{\epsilon 2}$ | 1.254 (0.002) | 1.302 (0.009) | intermediate, C−O(H) |
| $Glu159C^{\delta}-O^{\epsilon 1}$ | 1.252 (0.002) | 1.270 (0.021) | anionic |
| $Glu159C^{\delta}-O^{\epsilon 2}$ | 1.251 (0.004) | 1.272 (0.015) | anionic |
| | Assumed Distances for Each Case[b] | | |
| $C^{\delta}-O^{\epsilon 1}$ | 1.25 | 1.22 | |
| $C^{\delta}-O^{\epsilon 2}$ | 1.25 | 1.33 | |

[a] Values were obtained by averaging over the four monomers in the asymmetric unit; standard deviations are given in parentheses. [b] Distances assumed for each case are provided for comparison purposes.

In order to determine which of the above two possibilities best describes Glu69 in Q69E-$Fe^{2+}$SOD, we performed two parallel cycles of refinement against the X-ray diffraction data. In one, both Glu69 and Glu159 were refined against bond lengths appropriate for neutral Glu ($C^{\delta}-O^{\epsilon 1}$ = 1.22 Å, $C^{\delta}-O^{\epsilon 2}$ = 1.33 Å), whereas the second refinement assumed anionic Glu ($C^{\delta}-O^{\epsilon 1} = C^{\delta}-O^{\epsilon 2}$ = 1.25 Å) for both residues,[73] with Glu159 serving as an internal control. The *R*-values produced by the two refinements were identical. In both cases, the resulting two $C^{\delta}-O$ distances of Glu159 were indistinguishable, consistent with anionic glutamate (Table 4). This shows that our crystallographic data could over-ride the stereochemical restraints supplied by the model. In contrast, the $C^{\delta}-O$ distances of Glu69 refined to different values depending on which model was applied, and neither pair of refined distances adhered completely to the model. Thus, when defined as glutamate, the two refined $C^{\delta}-O$ distances were slightly unequal, yet when defined as glutamic acid the $C^{\delta}-O$ distances departed from the ideal values and approached each other (Table 4). This intermediate behavior suggests that Glu69 is partially protonated.

In the last cycle of refinement, Glu69 was defined as neutral (and Glu159 as anionic). None of the distances in the active site other than those internal to Glu69 itself were significantly different from the distances obtained using anionic Glu69 (supplemental Table S2). The final structure showed clear electron density concentrated at atoms (Figure 7), with solvent molecules that were very well-defined. However, we note that, in all of the four active sites, residual electron density not fully accounted for by the C, O, and N atoms was observed at 3 $\sigma$, between coordinated solvent, the $O^{\epsilon 2}$ of Glu69, and the $O^{\zeta}$ of Tyr34 (Figure 7, red mesh). Although the exact position of the extra density varied a bit among the four active sites, its distribution among the three O's suggests effective $H^+$ sharing among Tyr34, Glu69, and coordinated solvent, as this would tend to draw some electron density away from the proprietor O

(72) Carboxylates or carboxylic acids in which one O is H-bonded to water were identified in the Cambridge Structural Database. For 166 carboxylates receiving an H-bond from water, the average C−O distance for the H-bonded O was 1.24 Å (0.012) and the average C−O distance for the non-H-bonded O was 1.26 Å (0.012). These two distances are not significantly different, although there was a slight tendency for the O engaged in an H-bond to have a longer bond to C. In contrast, in 13 structures of neutral carboxylic acids donating an H-bond to water, the protonated O had an average C−O bond length that was 1.31 Å (0.015), more than 3 standard deviations longer than the double bonded C−O average distance of 1.22 Å (0.015), indicating localization of the double bond.

(73) Glu 159 was chosen as a control on the basis of its excellent electron density and low *B* values.

(74) DeLano, W. L. DeLano Scientific, San Carlos, CA, 2002.

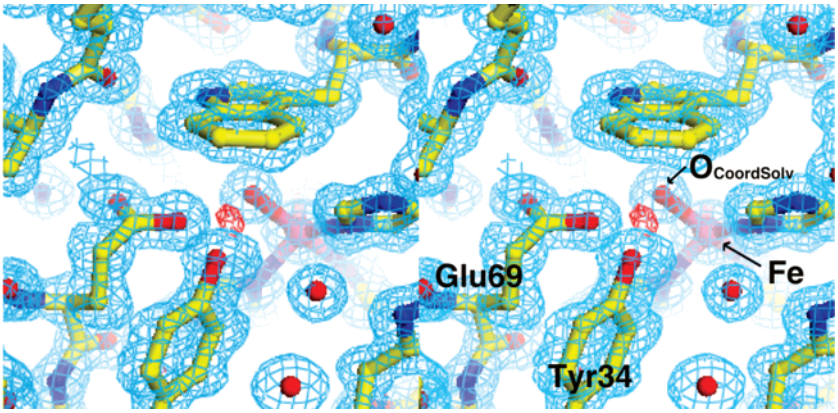


***Figure 7.*** Stereoview of the $2F_o-F_c$ electron density at 1 $\sigma$ (aqua mesh) and residual $F_o-F_c$ at 3 $\sigma$ (red mesh). The figure was generated using pymol.[74]

***Table 5.*** Distances among Active Site Residues in Models Optimized by DFT Calculations, from Different Starting Assumptions

| starting assumption → **distances after optimization** ↓ | A: GluOH/TyrOH/ CoordSolv=**OH**$^-$ | B: GluO$^-$/TyrOH/ CoordSolv=**H**$_2$O | C: GluOH/TyrO$^-$/ CoordSolv=**H**$_2$O | D: GluOH/TyrOH)/ CoordSolv=**H**$_2$O (channel solvent =**OH**$^-$)[a] |
|---|---|---|---|---|
| | | Bond Lengths (Å) | | |
| Fe—$O_{CoordSolv}$ | 2.269 | 2.266 | 2.266 | 2.275 |
| Glu69 $C^{\delta}$—$O^{\epsilon 1}$ (H-bonds to Trp122) | 1.254 | 1.256 | 1.254 | 1.251 |
| Glu69 $C^{\delta}$—$O^{\epsilon 2}$ (H-bonds to CoordSolv) | 1.317 | 1.316 | 1.316 | 1.321 |
| | | H-Bond Distances (Å) | | |
| $O_{CoordSolv}$ ··· $O^{\epsilon 2}{}_{Glu69}$ | 2.686 | 2.695 | 2.712 | 2.688 |
| $O_{CoordSolv}$ ··· $O^{\delta 1}{}_{Asp156}$ | 3.465 | 3.449 | 3.440 | 3.481 |
| $O^{\zeta}{}_{Tyr34}$ ··· $O^{\epsilon 2}{}_{Glu69}$ | 2.643 | 2.645 | 2.641 | 2.624 |
| $O^{\epsilon 1}{}_{Glu69}$ ··· $N^{\epsilon 1}{}_{Trp122}$ | 2.923 | 2.925 | 2.929 | 2.924 |

[a] An exogenous $OH^-$ was included in the substrate access channel in this model only, in the presence of neutral Glu69, Tyr34, and coordinated solvent. Upon refinement, a proton had been transferred to the channel solvent and lost from Glu69 to produce anionic Glu69, neutral Tyr34, and neutral coordinated solvent, as in the case of the other three models.

atoms toward the H-bonding partners. Thus, the data provide direct evidence for H-bonding between these residues, in addition to the good H-bonding distances separating the participating O atoms (Table 3). Such residual density evidence has not previously been available for an FeSOD, largely because existing FeSOD structures have not been refined to as high a resolution, possibly due to redox heterogeneity (see above), among other reasons. Since both Tyr34 and coordinated solvent conform well to neutral models, while our titrations indicate that one of the three active site residues is anionic, the intermediate refinement of Glu69 may represent anionic Glu69 partially protonated by H-bonds from coordinated $H_2O$ and Tyr34.

**Computational Evaluation of Alternative Interpretations of the Crystallographic Results.** We also used computations to assess the plausibility of various scenarios for the protonation states of active site residues in Q69E-$Fe^{2+}$SOD. Given the experimental evidence for an additional negative charge in the active site, relative to WT-$Fe^{2+}$SOD, we performed DFT geometry optimizations on Q69E-$Fe^{2+}$SOD active site models embodying four different possibilities for the identity of the additional anion: (A) coordinated solvent as $OH^-$ (instead of $H_2O$), (B) ionized Glu69, (C) ionized Tyr34, and (D) an exogenous $OH^-$ ion in the location of the crystallographic solvent molecule closest to the $Fe^{2+}$'s empty coordination site (see Table 5, supplemental Figure S4). Of these, A and C are excluded by the crystallographic results but serve as controls for the ability of the calculations to escape from incorrect starting assumptions. All four models converged to a final state in which Tyr34, coordinated solvent, and the exogenous solvent molecule (present only in model D), were neutral, based on the optimized positions of the H atoms. In all cases the converged structures contained ionized Glu69 (lacking a covalently bonded H atom).

The DFT optimized structures all display unequal C−O bond lengths for the side chain of Glu69, with the $O^{\epsilon 2}$ closest to coordinated solvent displaying a significantly longer bond of 1.32 Å, vs 1.26 Å for the C−O distance of the $O^{\epsilon 1}$ that faces Trp122 and Asn72. These compare well with the corresponding crystallographic distances of 1.30 vs 1.24 Å. Thus, the calculations confirm the possibility of unequal C−O bond distances, even when Glu69 is ionized.

**H-Bonding between Glu69 and Coordinated Solvent.** The DFT calculations also provide a possible explanation for an unexpected feature of the crystal structure: the $O_{CoordSolv}$—$O^{\epsilon 2}{}_{Glu69}$ distance is shorter than the $O_{CoordSolv}$—$O^{\delta 1}{}_{Asp156}$ distance. All the DFT calculations for which optimization produced an anionic Glu69, also displayed a *shorter* distance between Glu69 and coordinated solvent and a longer distance between coordinated solvent and Asp156 ($O_{CoordSolv}$—$O^{\epsilon 2}{}_{Glu69}$ = 2.7 Å, vs $O_{CoordSolv}$—$O^{\delta 1}{}_{Asp156}$ = 3.4 Å, Table 5). However DFT optimization yielded a *longer* Glu69-to-coordinated solvent distance and a shorter coordinated solvent-to-Asp156 distance for two other active site models in which the active site possessed neutral Glu 69 and the same overall charge as WT-FeSOD ($O_{CoordSolv}$—$O^{\epsilon 2}{}_{Glu69}$ = 3.0 Å vs $O_{CoordSolv}$—$O^{\delta 1}{}_{Asp156}$ = 2.9 Å).[75] This distinction reproduces one observed experimentally: when

residue 69 was neutral as in Q69H-FeSOD and the oxidized and reduced structures of WT-FeSOD, the $O_{CoordSolv}-O^{\epsilon 2}{}_{His/Gln69}$ distances were relatively long (3.4, 3.6 and 3.4 Å, respectively) and the $O_{CoordSolv}-O^{\delta 1}{}_{Asp156}$ distance was relatively short (3.0, 3.0, or 2.9 Å, respectively).[6,9] In contrast, the Q69E-$Fe^{2+}$SOD structure is characterized by a shorter $O_{CoordSolv}-O^{\epsilon 2}{}_{Glu69}$ distance and a longer $O_{CoordSolv}-O^{\delta 1}{}_{Asp156}$ distance (2.8 Å vs 3.2 Å, Table 3B, top two lines). We speculate that H-bond donation to coordinated solvent by a neutral residue 69 would reinforce a network in which coordinated solvent in turn donates an H-bond to Asp156. However anionic Glu69 would compete *against* Asp156 for H-bond acceptance from coordinated solvent so that an H-bond with Glu69 would occur at the expense of H-bonding with Asp156 to some extent.

Overall, based on DFT calculations, excess active site negative charge is most likely explained by ionization of Glu69, the observed crystallographic distances are better explained by anionic Glu69 than by a neutral residue 69, and the unequal $C^{\delta}-O$ bond lengths in Glu69's side chain are in fact *expected* in the circumstance of SOD's active site H-bond network, based on DFT calculations.

## Discussion

Mutation of Gln69 produces surprisingly large consequences for FeSOD. Q69H-FeSOD displays 30% WT activity and Q69E-FeSOD retains less than 1% of WT FeSOD activity, even though their 1.8 Å and 1.6 Å crystal structures, respectively, demonstrated that the overall protein structure was not significantly altered.[9] The mutants' decreased activities could be explained by an elevation of their $E_m$s by 220 mV for Q69H-FeSOD and apparently over 660 mV for Q69E-FeSOD, compared to WT-FeSOD.[9] However these changes in $E_m$ are very large, considering the chemically (Q to H) or structurally (Q to E) conservative natures of the mutations and their locations in the second coordination sphere of Fe.[9,76] Therefore, we now explore the possibilities that the elevated $E_m$s reflect altered Fe electronic structure, altered active site charge, or altered H-bonding and redox-coupled proton transfer.

**Electronic Structure and Ligand Environment of Fe.** The paramagnetically shifted NMR signals of reduced Q69H- and Q69E-$Fe^{2+}$SOD show that the active site structure, ligand field asymmetry, and covalency are similar to those of WT-$Fe^{2+}$-SOD. Similarly, for the oxidized states, the absorption and EPR spectra of Q69H-$Fe^{3+}$SOD are very similar to those of WT-$Fe^{3+}$SOD, indicating that the electronic structure, spin state, and overall coordination geometry of the active site $Fe^{3+}$ are not strongly perturbed upon mutation of Gln69 to His.

Even for Q69E-$Fe^{3+}$SOD, the reduced and oxidized states formed resemble species observed for WT-$Fe^{3+}$SOD. However, for Q69E-$Fe^{3+}$SOD, the WT-like pentacoordinate oxidized state is unstable at neutral pH compared to a six-coordinate state that we propose results from coordination of an exogenous anion (i.e., $OH^-$). Since formation of a six-coordinated state is spontaneous, this lowers the free energy of the oxidized state and the apparent $E_m$.[98] Thus, adoption of this state is not responsible for the high apparent $E_m$ of Q69E-FeSOD but rather makes it a *lower bound* for the $E_m$ of a redox couple linking pentacoordinate states. Consequently, our spectroscopic data indicate that the Fe coordination environment and electronic structure differences are unlikely to be the principal causes of the elevated $E_m$s of Q69H- and Q69E-FeSOD.

**Anion-Binding Affinities and p*K*'s: The Charge of Residue 69 in Q69H- and Q69E-FeSOD.** WT-FeSOD displays a p*K* near 9 in each oxidation state. The oxidized state p*K* reflects coordination of an exogenous $OH^-$ to $Fe^{3+}$,[2,13,64] whereas the reduced state p*K* corresponds to deprotonation of Tyr34.[15,62] Similar events were observed in Q69H-FeSOD, and the values of the corresponding p*K*s were relatively unchanged. Q69H-$Fe^{3+}$SOD's WT-like affinities for $F^-$ and $N_3^-$ also argue that the active site charge is like that of WT-$Fe^{3+}$SOD. These results are most consistent with His69 being neutral in both oxidation states.[77]

Glu69 does not appear to be ionized in the oxidized state, based on the elevated affinity of this state for anions. However a neutral Glu69 would not be favorable either, due to the low p*K* expected for a carboxyl group involved in the relatively polar network of H-bonds that surrounds Glu69. Thus, neutrality would be *enforced*, consistent with the instability of this state. Indeed, since coordinated solvent is almost certainly $OH^-$, it would tend to suppress ionization of Glu69, only ~3 Å away. Thus, we propose that Q69E-$Fe^{3+}$SOD has a neutral Glu69.

In the reduced state, Glu69 appears at least partially protonated based on its $C^{\delta}-O$ bond lengths. However, ionization of the active site Tyr34 is suppressed, as is base-catalyzed proton exchange for His160.[29] Both argue in favor of ionization of Glu69. Thus, the unequal $C^{\delta}-O$ bond lengths are probably the result of H-bonding that concentrates Glu69's negative charge on $O^{\epsilon 2}$ (closer to coordinated $H_2O$ and Tyr34) and lengthens that $C^{\delta}-O$ bond. This interpretation is supported by DFT geometry optimization which produced anionic Glu69, but with $C^{\delta}-O$ with bond distances very similar to the values obtained upon refinement of the crystallographic data assuming ~COOH. Indeed, the $O^{\epsilon 1}$ of Glu69 that faces Trp122 and Asn72 receives H-bonds from two neutral residues with p*K*s near 13 and 17, at distances of 2.85 (2) Å and 3.16 (5) Å, respectively. By contrast, the $O^{\epsilon 2}$ that faces coordinated solvent would receive H-bonds from a strongly polarized water molecule with a p*K* closer to 11[78] and a Tyr with a p*K* >10.8 but normally not greater than 13, at distances of 2.78 (1) and 2.78 (4) Å, respectively. Thus, based on criteria of p*K* matching as well as proximity, H-bonding to $O^{\epsilon 2}$ is expected to be stronger and to produce greater partial protonation than that experienced by $O^{\epsilon 1}$.

Finally, residual electron density was observed among coordinated solvent, the nearby $O^{\epsilon 2}$ of Glu69, and the $O^{\zeta}$ of Tyr34, suggesting proton sharing among these three (Figure 7). In contrast, there is no excess electron density greater than 1 $\sigma$ between Glu69's $O^{\epsilon 1}$ and its H-bonding partners. Thus, for reduced Q69E-$Fe^{2+}$SOD we favor a model in which formally ionized Glu69 accepts strong H-bonds from a combination of coordinated $H_2O$ and Tyr34, which effectively partially protonate and polarize Glu69.

(75) In both models, Tyr34, Glu69, and coordinated solvent were neutral. In one, Tyr34's hydroxyl H was directed toward Glu69 to donate an H-bond; in the other, Tyr34's hydroxyl H was directed away from Glu69 and Tyr34 accepted an H-bond from Glu69.

(76) While the residue mutated derives from the second sphere, one interpretation of our results is that altered H-bonding resulting from the mutation in effect changes the nature of a first sphere residue, from more $OH^-$-like to more $H_2O$-like.

(77) It is reasonable that the nearby net-positively charged Fe center would disfavor protonation of His69.

(78) Baes, C. F., Jr.; Mesmer, R. E. *The Hydrolysis of Cations*; John Wiley & Sons: New York, 1976; p 236.

***Scheme 2.*** Proposed Protonation States in the Active Site of Q69H-FeSOD[a]

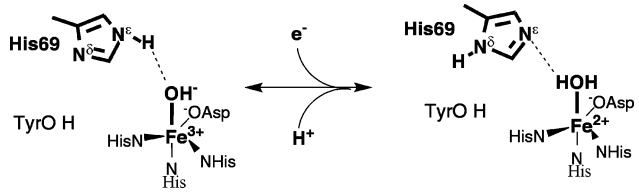


[a] Dashed lines represent hydrogen bonds, and solid lines represent bonds. Note that in the oxidized state the alternative tautomer of His69 cannot be excluded.

**Proposals for Changes in H-Bonding and Proton Transfer Relative to WT-FeSOD.** In Q69H-FeSOD, apparent retention of WT-like electronic structure for the Fe in both oxidation states indicates that coordinated solvent is $OH^-$ in the oxidized state and $H_2O$ in the reduced state, as in the case of WT-FeSOD. This indicates that either a proton is taken up upon reduction, as in WT-FeSOD,[2,79] or a nearby residue transfers a proton to coordinated solvent. His69 is excluded by our finding that it is neutral in both states. Tyr34 retains a WT-like p*K* near 9 in reduced Q69H-$Fe^{2+}$SOD, indicating that it has not released its proton at neutral pH. The ligand histidines also retain their exchangeable protons, as these can be observed by NMR spectroscopy (Figure 2). Thus, all the ionizable protons can be accounted for within the active site (Figure 1), and we propose that the coordinated $H_2O$ generated upon reduction of the metal center acquires its second proton from solvent, as in the case of WT-FeSOD (Scheme 2).

For oxidized Q69E-$Fe^{3+}$SOD, our data imply neutral Glu69.[80] However, Glu69 and coordinated solvent are expected to have similar intrinsic p*K*s in oxidized Q69E-$Fe^{3+}$SOD,[78] so it would be overly simplistic to construe one as fully protonated and the other as fully deprotonated, especially since Glu69 appears to develop a very strong H-bond with coordinated $OH^-$ based on MCD spectroscopic studies of Q69E-$Fe^{3+}$SOD's $N_3^-$ complex.[81] Thus, Glu69's labile proton might best be viewed as partially shared.[81,82]

For reduced Q69E-$Fe^{2+}$SOD, our experimental conclusions that Glu69 is at least partially ionized and that coordinated solvent is $H_2O$ are consistent with the expectation that the p*K* of solvent coordinated to $Fe^{2+}$ is much higher than that of solvent coordinated to $Fe^{3+}$, 11 vs 3.5 for formation of $OH^-$ as the second anionic ligand in Fe-aquo species.[83] Thus, coordinated solvent in $Fe^{2+}$SOD is expected to be $H_2O$ at neutral pH, which would allow Glu69 to ionize, in accordance with its intrinsic p*K* of 4.3 and relatively polar environment.[84,85] Hence, we propose Scheme 3 for H-bonding and $OH^-$ release in the active site of Q69E-FeSOD. Ionized Glu69 can explain part of the higher stability of reduced Q69E-$Fe^{2+}$SOD and, thus, part of Q69E-FeSOD's elevated $E_m$. The above inferences also argue that the H-bond between coordinated solvent and Glu69 would have the opposite polarity from the analogous one in WT-FeSOD: ionic $Glu69^-$ would *accept* an H-bond rather than donate one. This would tend to stabilize coordinated $H_2O$ more than $OH^-$ and thus favor the $Fe^{2+}$ state.

***Scheme 3.*** Proposed Protonation States in the Active Site of Q69E-FeSOD[a]

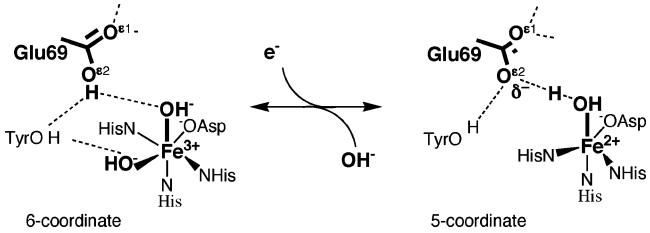


[a] Dashed lines represent hydrogen bonds, and solid lines represent bonds. In the reduced state, the H-bond between Glu69 and coordinated solvent is envisioned as involving significant sharing of the $H^+$ involved. (This may also be true of the oxidized state.)

In summary, for Q69E-FeSOD we *propose* that a proton is effectively shared between Glu69 and coordinated solvent and passes back and forth between them as the Fe cycles between oxidation states (Scheme 3).[86] Glu69 appears to be neutral in oxidized Q69E-$Fe^{3+}$SOD where coordinated solvent is most likely $OH^-$, while Glu69 is most likely anionic in reduced Q69E-$Fe^{2+}$SOD where coordinated solvent is $H_2O$. This proposal is consistent with DFT calculations. Geometry optimization of an active site model of Q69E-$Fe^{2+}$SOD with neutral Glu69 and coordinated $OH^-$ produced Q69E-$Fe^{2+}$SOD with anionic Glu69 and coordinated $H_2O$ (supplemental Table S3, Figure S4), demonstrating that our proposed internal proton transfer is reasonable on first principles. When internal proton transfer was prevented by fixing the OH bond lengths of Glu69 and Tyr34, the resulting Q69E-$Fe^{2+}$SOD with neutral Glu69 and coordinated $OH^-$ was associated with an $E_m$ many hundreds of millivolts lower than that obtained allowing internal proton transfer. When coordinated solvent was allowed to acquire a proton from solvent, an $E_m$ a few hundred millivolts more positive was obtained than that in the absence of proton transfer; however even this was many hundreds of millivolts lower than that produced by allowing proton transfer from Glu69. Thus, while the calculations do not quantitatively reproduce the observed $E_m$,[87] they indicate that protonation of coordinated solvent as well as acquisition of this proton from Glu69 can contribute strongly to an elevated $E_m$ for Q69E-FeSOD.

Because the NMR data reveal a WT-like reduced state, reduction appears to be accompanied by release of the proposed exogenous $OH^-$ to restore a WT-like pentacoordinate $Fe^{2+}$ site. In water, this is *formally* equivalent to $H^+$ uptake.[88] Thus, we also *propose* that Q69E-FeSOD *effectively* couples proton

(79) Definitive proof of proton coupled electron transfer awaits demonstration that the $E_m$ increases by 60 mV per unit decrease in pH.
(80) Q69E-$Fe^{3+}$SOD's high affinity for a sixth ligand could represent *effective* long-range ionization of hydrated Glu69, via the equilibrium: $Glu^- + H_2O \leftrightarrow GluH + OH^-$).
(81) Xie, J.; Yikilmaz, E.; Miller, A.-F.; Brunold, T. C. Personal communication.
(82) Shan, S.; Loh, S.; Herschlag, D. *Science* **1996**, *272* (5 April), 97−101.
(83) p*K*'s of metal-coordinated solvent are based on values in Baes for hexa-aquo compounds: for $Fe^{3+}$ the p*K*'s occur near 2.2, 3.5, 6 for formation of the mono-, di-, and tri-$OH^-$ complexes, whereas for $Fe^{2+}$ the analogous p*K*'s are approximately 9.5, 11.1, 10.4 (Baes, Hydrolysis of cations, 1976). Because the metal ion of SOD is coordinated by an $Asp^-$ ligand, we adopt the use of the second p*K* instead of the first. Thus for $Fe^{3+}$SOD we estimate that the coordinated solvent's p*K* is near 3.5 and for $Fe^{2+}$SOD we estimate a p*K* near 11. Both are consistent with experimental data on WT-FeSOD.
(84) Creighton, T. E. *Proteins: structures and molecular properties*, 2nd ed.; Freeman & Co.: 1993.
(85) Metzler, D. E. *Biochemistry. The chemical reactions of living cells*; Harcourt/Academic Press: San Diego, CA, 2001; Vol. 1.
(86) This is consistent with the fact that Glu's intrinsic p*K* falls between those of water coordinated to $Fe^{3+}$ and water coordinated to $Fe^{2+}$.
(87) We do not place strong emphasis on energies calculated for restrained models because they were not fully optimized. However an optimized model of the Q69E-FeSOD active site yielded an $E_m$ 400 mV higher than that of WT-FeSOD when both oxidized states were assumed to be pentacoordinate, for ease of comparison. Thus, simplifed active sites are able to reproduce a large fraction of the observed elevation of Q69E-FeSOD's $E_m$ relative to WT-FeSOD, lending credibility to the computational results, in general.
(88) However the free energy of dissociation of water must be taken into account when relating the energies of the two formulations.

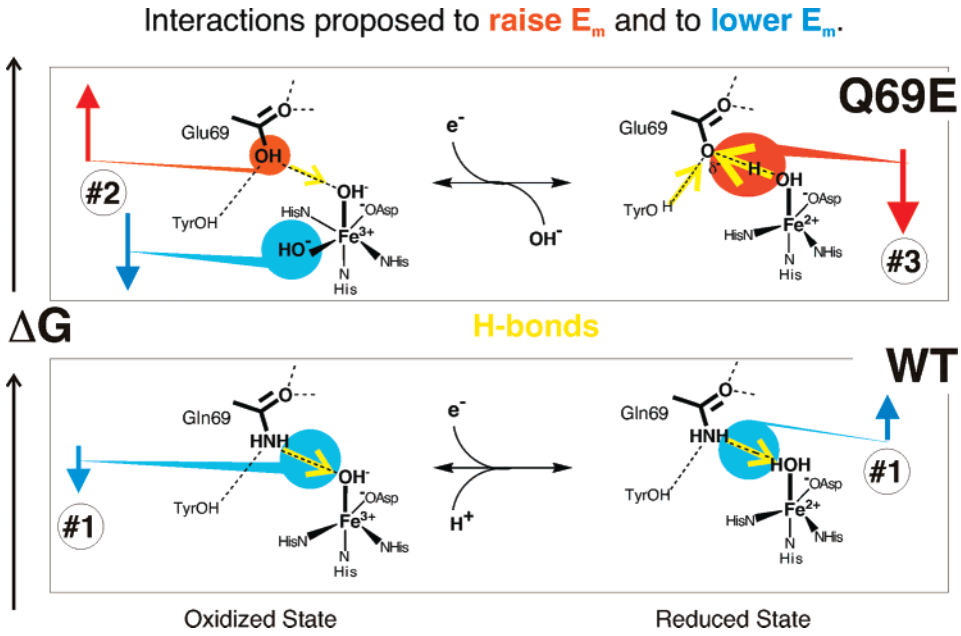


***Figure 8.*** Proposed interactions that may decrease (blue) or increase (red) the $E_m$. Arrows refer to contributions to the free energy of the oxidized (left) or reduced (right) states of WT-FeSOD (below) or Q69E-FeSOD (above). Circled numbers refer to the three proposed contributions to redox tuning discussed in the text.

uptake to metal ion reduction at neutral pH,[79] although the identities of the proton equivalents are different in Q69E-FeSOD than in WT- or Q69H-FeSOD (compare Schemes 2 and 3). Since the energetics of proton transfer contribute to the measured $E_m$, a viable proposal regarding proton transfer should be consistent with the elevated $E_m$ observed for Q69E-FeSOD and, moreover, could be crucial in explaining it.

**Contributions of Residue 69 to Redox Tuning.** The proposed protonation states and H-bonding in Scheme 3 support the possibility that modified H-bonding and proton transfer could alter the $E_m$ via the energetics of proton transfer. All the measurements needed for a quantitative prediction of the $E_m$ expected based on the model are not available at this time; nonetheless, with a few reasonable estimates, the plausibility of the model can be tested. The following discussion focuses on three redox tuning contributions indicated by the proposed changes in H-bonding and proton transfer.

*(1) Relief from H-bond donation to coordinated solvent that is enforced in WT-FeSOD.* In WT-FeSOD, Gln69 H-bonds with residues in different secondary structural elements and even different domains of FeSOD. The H-bond with Trp122 must constitute H-bond acceptance by Gln69 and therefore must involve the Gln69 $C^{\delta}{=}O^{\epsilon 1}$. This constrains the Gln69 $\sim N^{\epsilon 2}H_2$ to *donate* an H-bond to coordinated solvent (Figure 1).[6] Indeed, several Gln146 mutants of MnSOD are more stable than the WT enzyme,[25] indicating that the active site Gln's interactions may be enforced, rather than entirely favorable. Thus, the H-bond between Gln and coordinated solvent could actively modulate the coordinated solvent's p*K*. H-Bond donation will tend to favor coordinated $OH^-$ and, thus, the $Fe^{3+}$ state (Figure 8, lower panel).

It is difficult to quantify this effect in WT-FeSOD. However since Q69H-FeSOD behaves like WT-FeSOD in most ways but lacks the constraining H-bonds between Gln69 and Trp122, Tyr34, and Asn72,[89] the 220 mV increase in $E_m$ associated with the Q69H mutation provides an *estimate* of the redox tuning lost upon disruption of the H-bond network. Thus in WT-FeSOD, we estimate that enforcement of H-bond donation from Gln69 to coordinated solvent contributes roughly −220 mV to the $E_m$. This corresponds to approximately 7 kJ/mol for each of the three H-bonds lost in Q69H-FeSOD, which is consistent with literature values.[90−93]

*(2) Source of the redox-coupled proton.* In WT-FeSOD, where the coordinated solvent acquires a proton upon $Fe^{3+}$ reduction, the coordinated solvent's p*K*s in the oxidized and reduced enzyme contribute to the observed $E_m$.[24] Ease of protonating coordinated solvent translates into a higher $E_m$. Similarly in Q69E-$Fe^{2+}$SOD, the crystal structure indicates that coordinated solvent is protonated upon reduction of $Fe^{3+}$. However, our data show that Glu69 loses a proton, so $Fe^{3+}$ reduction appears coupled to *effective* transfer of a proton from Glu69 to coordinated solvent and dissociation of the exogenous $OH^-$ from the sixth coordination site[94] (Scheme 3). The former is more favorable than proton uptake from water, by an amount proportional to the difference between the p*K*s of water and Glu69 in Q69E-$Fe^{3+}$SOD.[95] Several factors affect the effective p*K* of Glu69, as well as the p*K*s of coordinated solvent (see Supporting Information). Nonetheless, even if we make the conservative estimate that only *half* of the possible advantage of transferring a proton from Glu instead of water persists, the $E_m$ is still expected to increase by some 340 mV (Figure 8 upper

(89) Q69H-FeSOD was found to retain a WT-like active site structure [Yikilmaz, et al. *Biochemistry* **2006**, *45*, 1151−1161].
(90) Fersht, A. *Structure and Mechanism in Protein Science*; Freeman and Co.: New York, 1999.
(91) Hammen, P. K.; Scholtz, J. M.; Anderson, J. W.; Waygood, E. B.; Klevit, R. E. *Protein Sci.* **1995**, *4*, 936−944.
(92) Kiefer, L. L.; Paterno, S. A.; Fierke, C. A. *J. Am. Chem. Soc.* **1995**, *117*, 6831−6837.
(93) Goodin, D. B.; McRee, D. E. *Biochemistry* **1993**, *32*, 3313−3324.
(94) Binding of an exogenous ligand to the oxidized state only would tend to lower $E_m$ and not raise it, so this is not considered further in our effort to understand the elevated $E_m$ of Q69E-FeSOD.
(95) Defining $pK_E^{ox}$ as the oxidized-state p*K* of Glu69, the increase in $E_m$ associated with drawing a proton from Glu69 instead of water depends on 2.3 RT/*F*(15.7 − $pK_E^{ox}$), where *R* and *F* are the ideal gas constant and Faraday's constant, 15.7 is the p*K* of water, and *T* is the absolute temperature. An *upper-limit* estimate can be obtained by using the p*K* glutamic acid in water, $pK_E^{ox}$ = 4.3, yielding 680 mV. More details are provided in the Supporting Information.

left).[95] This is consistent with the results of DFT calculations noted above.

*(3) Strong H-bond acceptance favoring coordinated $H_2O$ in Q69E-$Fe^{2+}$SOD.* The experimental evidence for ionized Glu69 accepting a strong H-bond from coordinated solvent indicates that the H-bond between coordinated $H_2O$ and residue 69 is reversed in reduced Q69E-$Fe^{2+}$SOD, compared to the case in WT-$Fe^{2+}$SOD. This would significantly stabilize coordinated $H_2O$ and raise Q69E-FeSOD's $E_m$. Based on the short $O^{\epsilon 2}{}_{Glu69} \cdots O_{CoordSolv}$ distance of 2.8 Å, residual electron density, and Glu69 $C^{\delta}-O$ bond lengths indicative of partial proton transfer, a relatively high energy of 20 kJ/mol $\approx$ 200 mV can be assigned to this H-bond and its strong supporting network[90,96] (Figure 8, upper right).

The sum of these three estimated contributions can *roughly* account for a 760 mV increase in $E_m$. This is large but comparable to the observed apparent minimum increase of 660 mV, indicating that the altered H-bonding and proton transfer proposed in Scheme 3 are compatible with the observed elevation in $E_m$. The investigations of Fe electronic structure, active site charge, and residue 69 protonation state reported above thus provide unique experimental support for a model in which H-bonding and the contributions of redox-coupled proton transfer can make a very strong contribution to the $E_m$.[23,24]

(96) Dey, A.; Hocking, R. K.; Larsen, P.; Borovik, A. S.; Hodgson, K. O.; Hedman, B.; Solomon, E. I. *J. Am. Chem. Soc.* **2006**, *128*, 9825−9833.
(97) The active site $E_m$ is proportional to the energy of the oxidized state minus that of the reduced state, of the active site.
(98) Based on approximate 50% population of a pentacoordinate state at pH 5 vs the pH of 7.4 used for $E_m$ measurements, coordination of exogenous $OH^-$ is expected to lower the observed $E_m$ by approximately 140 mV.

**Acknowledgment.** We thank Dr. Ed Snell for help collecting crystallographic data. A.-F.M. gratefully acknowledges support from the N.S.F. (MCB012599) and the Michael and Kate Bárány Young Investigator Award (Biophysical Society) for this work. G.B. thanks the N.A.S.A. (Grant NAG-1983) and the Nebraska Research Initiative for funding, and T.C.B. thanks the N.I.H. (GM64631).

**Supporting Information Available:** A brief description of methods used to produce the mutant SOD genes and the FeSOD proteins. A derivation and explanations of approximations made in estimating contributions to redox tuning. Three tables: one providing crystallographic refinement statistics, another comparing active site distances resulting from a refinement assuming anionic Glu69 bond lengths vs a refinement using neutral Glu69 bond lengths, and a third providing structural parameters of various Q69E-$Fe^{2+}$SOD active site models studied by DFT calculation. Four figures: one comparing the NMR spectra of Q69E-$Fe^{2+}$SOD's active site resonances at low and high pH, a second showing a ribbon diagram of Q69E-FeSOD, a third comparing the lengths of active site H-bonds and their precision in the current 1.1 Å Q69E-$Fe^{2+}$-SOD structure with those obtained in the previous 1.6 Å structure and the published WT-$Fe^{2+}$SOD structure, and a fourth showing selected Q69E-$Fe^{2+}$SOD active site models before and after DFT optimization (or restrained optimization). This material is available free of charge via the Internet at http://pubs.acs.org.

JA069224T